

A two-stage two-derivative fourth order positivity-preserving discontinuous Galerkin method for hyperbolic conservation laws

Tianjiao Li¹, Juan Cheng², and Chi-Wang Shu³

Abstract

In this paper, a fourth order positivity-preserving (PP) scheme for hyperbolic conservation laws based on the two-stage two-derivative fourth order ($S_2D_2O_4$) time discretization and discontinuous Galerkin (DG) spatial discretization is developed. We construct a local Lax–Friedrichs type PP flux in the sense that the DG scheme with this flux satisfies the PP property. We use the strong stability preserving (SSP) $S_2D_2O_4$ time discretization and obtain the PP conditions for one-dimensional scalar conservation laws. With a PP limiter introduced in [X. Zhang and C.-W. Shu, *J. Comput. Phys.*, 229 (2010), pp.3091–3120], the SSP $S_2D_2O_4$ DG schemes are rendered preserving the positivity without losing conservation or high order accuracy. We carry out the extension of the method to two dimensions on rectangular meshes. Based on this idea, we further develop high-order DG schemes which can preserve the positivity of density and pressure for compressible Euler equations. Numerical tests for this fourth order DG scheme are reported to demonstrate the effectiveness of the algorithms.

Keywords: Hyperbolic conservation laws, Two-stage two-derivative fourth order ($S_2D_2O_4$) time discretization, Strong stability preserving (SSP), Positivity-preserving (PP), Discontinuous Galerkin (DG) method.

¹Graduate School, China Academy of Engineering Physics, Beijing 100088, China. E-mail: litianjiao22@gscaep.ac.cn.

²Corresponding author. Laboratory of Computational Physics, Institute of Applied Physics and Computational Mathematics, Beijing 100088, China and HEDPS, Center for Applied Physics and Technology, and College of Engineering, Peking University, Beijing 100871, China. E-mail: cheng_juan@iapcm.ac.cn. Research is supported in part by National Key R&D Program of China No. 2023YFA1009003, and NSFC grant 12031001.

³Division of Applied Mathematics, Brown University, Providence, RI 02912. E-mail: chi-wang_shu@brown.edu. Research is supported in part by NSF grant DMS-2309249.

1 Introduction

Hyperbolic conservation laws are basic tools to characterize the phenomena of flow and transport, e.g. the Burgers equation for traffic flow and the Buckley-Leverett equation for two phase flow as the scalar cases, and the Euler equations for compressible gas dynamics and shallow water equations for water with shallow depth as the system cases.

For scalar conservation laws, the solution satisfies the maximum-principle-satisfying (MPS) property, e.g. for the one dimensional scalar equation

$$u_t + f(u)_x = 0, \quad x \in \mathbb{R}, t > 0 \tag{1.1}$$

with initial condition

$$u(x, 0) = u_0(x), \quad x \in \mathbb{R}$$

the entropy solution satisfies $m \leq u(x, t) \leq M, \forall x \in \mathbb{R}, t > 0$, where $m = \min_{x \in \mathbb{R}} u_0(x)$ and $M = \max_{x \in \mathbb{R}} u_0(x)$. Same results also hold for periodic boundary conditions, bounded domain with compactly supported solution, and higher dimensions. For hyperbolic conservation law systems, the positivity of certain important physical quantities are satisfied by some hyperbolic systems, e.g. for the compressible Euler equations of gas dynamics, the positivity of density and pressure must be preserved.

Discontinuous Galerkin (DG) methods are widely used to compute conservation laws because of their high order accuracy, flexibility in complex geometries, and simplicity of parallelization, and have become one of the most common choices for developing bound-preserving solutions. In 1970, the first DG method for solving the steady linear transport problem was proposed by Reed et al. [32]. Cockburn et al. developed it into the Runge-Kutta discontinuous Galerkin Method (RKDG) in a series of papers [5–9] to solve nonlinear hyperbolic conservation laws. Limiters such as the total variation bounded (TVB) limiter [35] are usually used to stabilize the solution near shocks after each Runge-Kutta stage. Also, there are finite volume and finite difference methods used in the computation of conservation laws, e.g. [1, 20, 44, 52].

In order to achieve high-order accuracy, the semi-discrete DG scheme needs to be combined with time discretization, which ideally should have the same order of accuracy as the spatial discretization. The widely used Runge-Kutta (RK) method was first proposed by Carl Runge and Wilhelm Kutta around 1900 and applied to solve ordinary differential equations and then applied to solve partial differential equations [41] later. In [15, 16, 36], a strong stability preserving Runge-Kutta (SSP-RK) method (termed TVD time discretization in early work) was proposed, one of which is the widely used third-order accurate SSP-RK method. The SSP methods are convex combinations of forward Euler time discretization, which greatly simplify the proof of bound preservation as the analysis needs to be carried out only for the forward Euler time stepping. Another time discretization method, namely the Lax-Wendroff type method, is also widely used in the computation of time-dependent partial differential equations, for instance, the combination of Lax-Wendroff type time discretization with DG (LWDG) methods [17, 28, 30] or with the WENO schemes [29, 31], the arbitrary high order derivative Riemann problem (ADER) approach [13, 14, 39], and its variant based on the Galerkin space-time predictor [2, 11, 12], etc. The Lax-Wendroff type method utilizes information from partial differential equations by replacing the time derivatives with spatial derivatives in the Taylor expansion of the time variable. As a result, the Lax-Wendroff type method is a single-stage, explicit and higher order method that requires only one stabilizing scaling limiter per time step. However, the introduction of higher order derivatives leads to a complicated algorithm, both in the formulation and in its programming, especially when solving high dimensional systems of equations. Later, in order to synthesize the advantages and disadvantages of the two approaches, Christlieb et al. [4, 33] combined the Runge-Kutta method and the Lax-Wendroff type method to design multistage multiderivative time discretization methods, among which one of the popular time discretization is a two-stage two-derivative fourth order ($S_2D_2O_4$) time discretization method, requiring only two stages to reach the fourth order accuracy, and has fewer higher order derivative terms compared to the standard Lax-Wendroff type method. There have been many applications related to the

$S_2D_2O_4$ method in the last decade, for instance, the gas-kinetic schemes (GKS) [25, 26] and the HWENO schemes [20].

To ensure the robustness and stability of the numerical algorithm, strict preservation of physical bounds of the solution is important, since once the quantity is outside its physical range, the hyperbolicity of the equation may be lost, which often leads to simulation failure. Bound-preserving numerical methods for hyperbolic conservation laws have been intensively studied. Almost all of the time discretizations in the bound-preserving methods are based on Runge-Kutta or multi-step methods. In 2010, the DG spatial discretization and explicit time discretization methods for hyperbolic conservation laws were first investigated by Zhang and Shu with the help of weak monotonicity in the finite volume format [51, 52], who constructed a high-order positivity-preserving (PP) DG scheme for the convection equations and Euler equations by proving the cell average PP property and by using the PP limiter. Later, Wu and Shu proposed a general framework, called geometric quasilinearization (GQL) [45], for studying bound-preserving problems with nonlinear constraints. Besides, there are also many other methods, such as the flux limiter [21, 38, 46, 47], convex limiting [18, 19], optimization-based approaches [23, 42], etc. In addition to the explicit methods, there are also studies on backward Euler time discretization [22, 27]. Works mentioned above are mostly based on the Runge-Kutta or multi-step time discretizations.

In the study of the PP DG algorithm based on the Lax-Wendroff type discretization method, Moe et al. first designed a flux limiter and achieved the positivity of the one-stage third-order LW DG for the compressible Euler equations [24], and later, Xu and Shu developed the third order MPS direct DG (DDG) methods for convection-diffusion equations to the one-stage third-order LW DG method [48] to construct a PP algorithm for hyperbolic conservation laws. The current PP DG algorithms of conservation laws for the Lax-Wendroff type method only go up to the third-order accuracy.

For the study of PP DG algorithms for the diffusion equations, the authors in [53] proved that the ultra-weak DG, interior penalty (IP) DG, and traditional LDG schemes can only

achieve second-order PP property. Chen et al. used the direct DG (DDG) discretization method to make the DG schemes satisfy third-order PP property under special parameters [3], and Du and Yang applied the LDG method on dual mesh to achieve the same PP conclusion [10]. All the above conclusions are proved theoretically, but only up to third order accuracy. In 2012, Zhang et al. proposed a nonconventional fifth order finite volume WENO scheme which can be proved MPS for convection-diffusion equations [50]. In 2017, Zhang designed a class of local Lax-Friedrichs (LF) type PP flux for the compressible NS equations, and numerical experiments observed fourth order and higher order accuracy [49]. Srinivasan et al. reduced the PP flux to the LDG method for convection-diffusion equations, which can numerically achieve up to at least k -th order for polynomials of degree k , with k maximally tested to 5, for a specific class of problems [37]. All the above works are based on the Runge-Kutta time discretization.

So far, there seems to have no research on bound-preserving techniques for multistep multiderivative time discretizations such as the $S_2D_2O_4$ time discretization schemes. In this paper, we adopt the DG methods for the spatial discretization of the derivatives with the $S_2D_2O_4$ time discretization. In our work, we use the framework in [52], hence the high order accuracy of our approach is easy to guarantee. First, for the one-dimensional hyperbolic conservation law equation, the spatial derivative term in the $S_2D_2O_4$ time discretization schemes is discretized with reference to the LWDG discretization method proposed by Qiu et al. [30]. After that, a suitable PP flux is designed with reference to the idea about the flux design for the high-order PP LDG method in [37, 49], and the SSP form of the $S_2D_2O_4$ method [4] is considered, which is written in the form of a convex combination of provably bound-preserving terms and hence guarantees bound-preserving of the cell averages. Finally, the PP limiter proposed by Zhang and Shu [52] is applied to further make the whole solution positive-preserving. The algorithm is then generalized to the Euler equations and further to the two dimensional cases.

The rest of the paper is organized as follows. In Section 2, we introduce the strong

stability preserving (SSP) $S_2D_2O_4$ time-stepping scheme. In Section 3, we construct the PP $S_2D_2O_4$ DG methods for scalar conservation laws in one and two dimensional spaces, respectively. In Section 4, we further establish the PP $S_2D_2O_4$ DG schemes for the Euler equations in one and two dimensional spaces, respectively. The PP limiters are introduced in Section 5 to ensure the positivity of the whole numerical solution. In Section 6, we give extensive numerical examples to verify the effectiveness of our algorithms. In the end, we give some concluding remarks in Section 7.

2 $S_2D_2O_4$ time discretization

Consider the following time-dependent equation,

$$\frac{\partial u}{\partial t} = F(u).$$

Suppose we have already reached at the time $t = t_n$

$$u(t)|_{t=t_n} = u^n.$$

Here, F is an operator for spatial derivatives and u is the numerical solution. We consider the SSP $S_2D_2O_4$ time-stepping scheme [4]:

$$\begin{aligned} u^* &= \left(1 - \frac{4rK^2 + r^2}{8K^2}\right) u^n + \frac{r}{2} \left(u^n + \frac{\Delta t}{r} F(u^n)\right) + \frac{r^2}{8K^2} \left(u^n + \frac{K^2}{r^2} \Delta t^2 \dot{F}(u^n)\right) \\ &= \left(1 - \frac{4rK^2 + r^2}{8K^2}\right) u^n + \frac{r}{2} M_1 + \frac{r^2}{8K^2} M_2 \end{aligned} \quad (2.1a)$$

$$\begin{aligned} u^{n+1} &= r \left(1 - \frac{r^2}{6K^2}\right) \left(u^n + \frac{\Delta t}{r} F(u^n)\right) + \frac{r^2(4K^2 - r^2)}{24K^4} \left(u^n + \frac{K^2}{r^2} \Delta t^2 \dot{F}(u^n)\right) \\ &\quad + \frac{r^2}{3K^2} \left(u^* + \frac{K^2}{r^2} \Delta t^2 \dot{F}(u^*)\right) \\ &= r \left(1 - \frac{r^2}{6K^2}\right) M_1 + \frac{r^2(4K^2 - r^2)}{24K^4} M_2 + \frac{r^2}{3K^2} M_3 \end{aligned} \quad (2.1b)$$

where $\dot{F} = F_t$, $M_1 = u^n + \frac{\Delta t}{r} F(u^n)$, $M_2 = u^n + \frac{K^2}{r^2} \Delta t^2 \dot{F}(u^n)$, $M_3 = u^* + \frac{K^2}{r^2} \Delta t^2 \dot{F}(u^*)$ and the parameter K is in the restricted time step of preserving the following stability:

$$\left\| u^n + \Delta t^2 \dot{F}(u^n) \right\| \leq \|u^n\| \quad \text{for} \quad \Delta t \leq K \Delta t_{\text{FE}}$$

with Δt_{FE} being the time step restriction of preserving stability of Euler forward time:

$$\|u^n + \Delta t F(u^n)\| \leq \|u^n\| \quad \text{for} \quad \Delta t \leq \Delta t_{\text{FE}},$$

and the SSP coefficient r is given by the smallest positive root of the equation:

$$r^4 + 4K^2r^3 - 12K^2r^2 - 24K^4r + 24K^4 = 0.$$

In this scheme (2.1), u^* is the convex combination of u_j , M_1 and M_2 , and u^{n+1} is the convex combination of M_1 , M_2 and M_3 . Then according to the SSP property, the analysis for the positivity of conservation laws only needs to be carried out on the positivity of $u^n + \frac{\Delta t}{r}F(u^n)$, $u^n + \frac{K^2}{r^2}\Delta t^2\dot{F}(u^n)$ and $u^* + \frac{K^2}{r^2}\Delta t^2\dot{F}(u^*)$, which brings convenience to the proof of positivity.

3 The PP $S_2D_2O_4$ DG scheme for the scalar conservation laws

In this section, we study the PP $S_2D_2O_4$ DG methods for scalar conservation laws. Our framework for the proof of the PP property is based on [52], that is, we focus on proving the positivity of the cell averages of the solution, i.e. $\bar{u}^{n+1} \geq 0$, provided $u^n \geq 0$, where the superscripts n and $n + 1$ denote the time level t^n and t^{n+1} , respectively. After that, the PP limiter introduced in Section 5 will make the whole solution positive while maintaining high order accuracy and conservation.

For simplicity, we only discuss the one and two dimensional problems with periodic boundary conditions on uniform meshes, but the algorithms can be directly extended to three space dimensions and non-periodic cases with non-uniform meshes.

3.1 The PP $S_2D_2O_4$ DG scheme for 1D scalar conservation laws

Consider the scalar conservation laws in one dimension

$$u_t + f(u)_x = 0. \tag{3.1}$$

According to the information of the equation, we give the expressions of u_t and u_{tt} as follows:

$$\begin{aligned} u_t &= -f(u)_x = -f'(u)u_x, \\ u_{tt} &= -(f'(u)u_t)_x = (f'^2(u)u_x)_x. \end{aligned}$$

In the one dimensional space, we assume the domain $\Omega = [a, b]$ is discretized by $a = x_{\frac{1}{2}} < x_{\frac{3}{2}} < \dots < x_{N+\frac{1}{2}} = b$, and denote by $I_j = [x_{j-\frac{1}{2}}, x_{j+\frac{1}{2}}]$ the cells on Ω for $j = 1, 2, \dots, N$. Moreover, we denote the length of the cell I_j by $\Delta x_j = x_{j+\frac{1}{2}} - x_{j-\frac{1}{2}}$ and the time step $\Delta t = t^{n+1} - t^n$. We only consider uniform meshes in this section, i.e. $\Delta x_j \equiv \Delta x$, for $j = 1, \dots, N_x$. The finite element space in the DG schemes is taken as $V = \left\{ v \in L^2 : v|_{I_j} \in P^3(I_j), j = 1, 2, \dots, N \right\}$ where $P^3(I)$ is the space of polynomials of degree ≤ 3 in the cell I_j . Moreover, we denote the average of v at $x_{j+\frac{1}{2}}$ by $\{v\}_{j+\frac{1}{2}} = \frac{1}{2} \left(v_{j+\frac{1}{2}}^- + v_{j+\frac{1}{2}}^+ \right)$ and the jump of v at $x_{j+\frac{1}{2}}$ by $[v]_{j+\frac{1}{2}} = (v_{j+\frac{1}{2}}^+ - v_{j+\frac{1}{2}}^-)$.

We use the Gauss-Lobatto quadrature of $2N_q - 1$ points to evaluate integrals in one dimensional cells, where N_q is taken such that the fourth order accuracy is attained in the scheme, e.g. $N_q = 5$. We denote the Gauss-Lobatto quadrature points in I_j as $\{\hat{x}_j^\mu, \mu = 1, \dots, 2N_q - 1\}$, and let $\{\hat{\omega}_\mu, \mu = 1, \dots, 2N_q - 1\}$ be the corresponding quadrature weights satisfying $\sum_{\mu=1}^{2N_q-1} \hat{\omega}_\mu = 1$. In particular, $\hat{x}_j^1 = x_{j-\frac{1}{2}}, \hat{x}_j^{N_q} = x_j$ and $\hat{x}_j^{2N_q-1} = x_{j+\frac{1}{2}}$. We denote $\hat{u}_j^\mu = u(\hat{x}_j^\mu)$, for $\mu = 1, \dots, 2N_q - 1$.

In the 1D scalar conservation laws, the DG scheme is designed according to the SSP $S_2D_2O_4$ time-stepping scheme (2.1):

$$\int_{I_j} u_j^* v_h dx = \int_{I_j} \left(\left(1 - \frac{4rK^2 + r^2}{8K^2} \right) u_j^n + \frac{r}{2} M_1 + \frac{r^2}{8K^2} M_2 \right) dx, \quad \forall v_h \in V \quad (3.2a)$$

$$\int_{I_j} u_j^{n+1} v_h dx = \int_{I_j} \left(r \left(1 - \frac{r^2}{6K^2} \right) M_1 + \frac{r^2(4K^2 - r^2)}{24K^4} M_2 + \frac{r^2}{3K^2} M_3 \right) dx, \quad \forall v_h \in V \quad (3.2b)$$

For $M_1 = u_j^n + \frac{\Delta t}{r} F(u_j^n) = u_j^n - \frac{\Delta t}{r} (f(u_j^n))_x$, the corresponding DG scheme at the time level t^n is to find $M_1 \in V$, s.t. $\forall v_h \in V$,

$$\int_{I_j} M_1 v_h dx = \int_{I_j} u_j^n v_h dx + \frac{\Delta t}{r} \left(\int_{I_j} f(u_j^n) (v_h)_x dx - \hat{f}_{j+\frac{1}{2}}^{\text{LF}} (v_h)_{j+\frac{1}{2}}^- + \hat{f}_{j-\frac{1}{2}}^{\text{LF}} (v_h)_{j-\frac{1}{2}}^+ \right) \quad (3.3)$$

where $\hat{f}_{j+\frac{1}{2}}^{\text{LF}}$ is the numerical flux at $x_{j+\frac{1}{2}}$ defined as

$$\hat{f}_{j+\frac{1}{2}}^{\text{LF}} = \{f\}_{j+\frac{1}{2}} - \frac{\alpha}{2}[u]_{j+\frac{1}{2}}, \quad \alpha = \max_u |f'(u)| \quad (3.4)$$

which is the LF flux as used in [52].

For $M_2 = u_j^n + \frac{K^2}{r^2} \Delta t^2 \dot{F}(u_j^n) = u_j^n - \frac{K^2}{r^2} \Delta t^2 H_x(u_j^n)$ where $H = -f'(u)^2 u_x$, the DG scheme at the time level t^n is to find $M_2 \in V$, s.t. $\forall v_h \in V$,

$$\int_{I_j} M_2 v_h dx = \int_{I_j} u_j^n v_h dx + \frac{K^2}{r^2} \Delta t^2 \left(\int_{I_j} H(u_j^n) (v_h)_x dx - \hat{H}_{j+\frac{1}{2}}(v_h)_{j+\frac{1}{2}}^- + \hat{H}_{j-\frac{1}{2}}(v_h)_{j-\frac{1}{2}}^+ \right) \quad (3.5)$$

holds for $j = 1, 2, \dots, N$, where $\hat{H}_{j+\frac{1}{2}}$ is the numerical flux at $x_{j+\frac{1}{2}}$ which is defined similar to the flux in [37]:

$$\hat{H}_{j+1/2} = \frac{1}{2} \left(H_{j+1/2}^- + H_{j+1/2}^+ - \alpha_{j+\frac{1}{2}} \left(u_{j+1/2}^+ - u_{j+1/2}^- \right) \right), \quad (3.6)$$

where the penalty parameter $\alpha_{j+\frac{1}{2}}$ is defined to achieve the PP property for the scheme (3.5):

$$\alpha_{j+\frac{1}{2}} = \begin{cases} \max \left\{ \left| \frac{H_{j+\frac{1}{2}}^+}{u_{j+\frac{1}{2}}^+} \right|, \left| \frac{H_{j+\frac{1}{2}}^-}{u_{j+\frac{1}{2}}^-} \right| \right\}, & \text{if } u_{j+\frac{1}{2}}^+ \neq 0 \text{ and } u_{j+\frac{1}{2}}^- \neq 0, \\ \left| \frac{H_{j+\frac{1}{2}}^+}{u_{j+\frac{1}{2}}^+} \right|, & \text{if } u_{j+\frac{1}{2}}^+ \neq 0 \text{ and } u_{j+\frac{1}{2}}^- = 0, \\ \left| \frac{H_{j+\frac{1}{2}}^-}{u_{j+\frac{1}{2}}^-} \right|, & \text{if } u_{j+\frac{1}{2}}^+ = 0 \text{ and } u_{j+\frac{1}{2}}^- \neq 0, \\ 0 & \text{if } u_{j+\frac{1}{2}}^+ = 0 \text{ and } u_{j+\frac{1}{2}}^- = 0. \end{cases} \quad (3.7)$$

For $M_3 = u_j^* + \frac{K^2}{r^2} \Delta t^2 \dot{F}(u_j^*) = u_j^* - \frac{K^2}{r^2} \Delta t^2 H_x(u_j^*)$, the DG scheme is similar to (3.5) and the numerical flux $\hat{H}_{j+\frac{1}{2}}^*$ at $x_{j+\frac{1}{2}}$ is defined as

$$\hat{H}_{j+1/2}^* = \frac{1}{2} \left(H_{j+1/2}^{*-} + H_{j+1/2}^{*+} - \beta_{j+\frac{1}{2}} \left(u_{j+1/2}^{*+} - u_{j+1/2}^{*-} \right) \right), \quad (3.8)$$

where the penalty parameter $\beta_{j+\frac{1}{2}}$ has the similar definition as $\alpha_{j+\frac{1}{2}}$:

$$\beta_{j+\frac{1}{2}} = \begin{cases} \max \left\{ \left| \frac{H_{j+\frac{1}{2}}^{*+}}{u_{j+\frac{1}{2}}^{*+}} \right|, \left| \frac{H_{j+\frac{1}{2}}^{*-}}{u_{j+\frac{1}{2}}^{*-}} \right| \right\}, & \text{if } u_{j+\frac{1}{2}}^{*+} \neq 0 \text{ and } u_{j+\frac{1}{2}}^{*-} \neq 0, \\ \left| \frac{H_{j+\frac{1}{2}}^{*+}}{u_{j+\frac{1}{2}}^{*+}} \right|, & \text{if } u_{j+\frac{1}{2}}^{*+} \neq 0 \text{ and } u_{j+\frac{1}{2}}^{*-} = 0, \\ \left| \frac{H_{j+\frac{1}{2}}^{*-}}{u_{j+\frac{1}{2}}^{*-}} \right|, & \text{if } u_{j+\frac{1}{2}}^{*+} = 0 \text{ and } u_{j+\frac{1}{2}}^{*-} \neq 0, \\ 0 & \text{if } u_{j+\frac{1}{2}}^{*+} = 0 \text{ and } u_{j+\frac{1}{2}}^{*-} = 0. \end{cases} \quad (3.9)$$

Theorem 3.1. For the fourth order $S_2D_2O_4$ DG scheme of the one dimensional scalar conservation laws using the fluxes (3.4), (3.6) and (3.8), if the following conditions are satisfied:

1. All point values at the Gauss-Lobatto quadrature points are non-negative, i.e. $\hat{u}_j^\mu \geq 0$ for $\mu = 1, \dots, 2N_q - 1$ and all j , which include $u_{j\pm\frac{1}{2}}^\pm$.

2. For all j , $H_{j+\frac{1}{2}}^\pm = 0$ if $u_{j+\frac{1}{2}}^\pm = 0$.

Then the cell averages $\bar{u}_j^{n+1} \geq 0$ under the time step constraint below,

$$\frac{\Delta t}{\Delta x} \max_j \left| f' \left(u_{j+\frac{1}{2}}^\pm \right) \right| \leq r\hat{\omega}_1, \quad \frac{\Delta t^2}{\Delta x^2} \max_j \left\{ \alpha_{j+\frac{1}{2}}, \beta_{j+\frac{1}{2}} \right\} \leq \frac{r^2}{K^2} \hat{\omega}_1$$

where $\alpha_{j+\frac{1}{2}}$ is defined as in (3.7) and $\beta_{j+\frac{1}{2}}$ is defined as in (3.9).

Proof. We take the test function $v_h = 1$ on I_j and zero anywhere else in the scheme (3.2), and denote $\lambda = \frac{\Delta t}{\Delta x}$, then we obtain the formula satisfied by the cell average of u^* in the cell I_j ,

$$\bar{u}_j^* = \left(1 - \frac{4rK^2 + r^2}{8K^2} \right) \bar{u}_j^n + \frac{r}{2} R_1 + \frac{r^2}{8K^2} R_2 \quad (3.10)$$

where

$$R_1 = \left(\bar{u}_j^n - \frac{\lambda}{r} \hat{f}_{j+\frac{1}{2}}^{\text{LF}} + \frac{\lambda}{r} \hat{f}_{j-\frac{1}{2}}^{\text{LF}} \right)$$

$$R_2 = \left(\bar{u}_j^n - \frac{K^2}{r^2} \lambda^2 \hat{H}_{j+\frac{1}{2}} + \frac{K^2}{r^2} \lambda^2 \hat{H}_{j-\frac{1}{2}} \right)$$

and

$$\bar{u}_j^n = \sum_{\mu=1}^{2N_q-1} \hat{w}_\mu u_j(\hat{x}_j^\mu) \quad (3.11)$$

Since R_1 has exactly the same form as in [52], we have $R_1 \geq 0$ under the condition $\lambda \leq \frac{r\hat{\omega}_1}{\max_j \left| f' \left(u_{j+\frac{1}{2}}^\pm \right) \right|}$. Now we rewrite R_2 by (3.11) and (3.6),

$$R_2 = \sum_{\mu=2}^{2N_q-2} w_\mu u_j(\hat{x}_j^\mu) + u_{j-\frac{1}{2}}^+ \left[w_1 - \frac{K^2}{2r^2} \lambda^2 \alpha_{j-\frac{1}{2}} + \frac{K^2}{2r^2} \lambda^2 \frac{H_{j-\frac{1}{2}}^+}{u_{j-\frac{1}{2}}^+} \right]$$

$$+ u_{j+\frac{1}{2}}^- \left[w_{2N_q-1} - \frac{K^2}{2r^2} \lambda^2 \alpha_{j+\frac{1}{2}} - \frac{K^2}{2r^2} \lambda^2 \frac{H_{j+\frac{1}{2}}^-}{u_{j+\frac{1}{2}}^-} \right] \quad (3.12)$$

$$+ \frac{K^2}{2r^2} \lambda^2 u_{j-\frac{1}{2}}^- \left[\alpha_{j-\frac{1}{2}} + \frac{H_{j-\frac{1}{2}}^-}{u_{j-\frac{1}{2}}^-} \right] + \frac{K^2}{2r^2} \lambda^2 u_{j+\frac{1}{2}}^+ \left[\alpha_{j+\frac{1}{2}} - \frac{H_{j+\frac{1}{2}}^+}{u_{j+\frac{1}{2}}^+} \right]$$

For the right hand side in (3.12) to be a positive linear combination of point values $u_{j\pm\frac{1}{2}}^\pm$ and $u_j(\widehat{x}_j^\mu)$, it suffices to require $H = 0$ wherever $u = 0$ and the time step to satisfy the following constraint (notice that $\widehat{\omega}_1 = \widehat{\omega}_{2N_q-1}$):

$$\frac{K^2}{2r^2} \max_j \left\{ \alpha_{j+\frac{1}{2}} + \frac{H_{j+\frac{1}{2}}^-}{u_{j+\frac{1}{2}}^-}, \alpha_{j-\frac{1}{2}} - \frac{H_{j-\frac{1}{2}}^+}{u_{j-\frac{1}{2}}^+} \right\} \lambda^2 \leq \widehat{\omega}_1.$$

According to the definition of $\alpha_{j+\frac{1}{2}}$ in (3.7), $\left| \alpha_{j+\frac{1}{2}} + \frac{H_{j+\frac{1}{2}}^-}{u_{j+\frac{1}{2}}^-} \right| \leq 2\alpha_{j+\frac{1}{2}}$ and $\left| \alpha_{j-\frac{1}{2}} - \frac{H_{j-\frac{1}{2}}^+}{u_{j-\frac{1}{2}}^+} \right| \leq 2\alpha_{j-\frac{1}{2}}$, and then the time step condition above can be further simplified as the following CFL condition for an explicit scheme:

$$\frac{K^2}{r^2} \lambda^2 \max_j \alpha_{j+\frac{1}{2}} \leq \widehat{\omega}_1. \quad (3.13)$$

Therefore, we have $R_2 \geq 0$ under this time step condition and then combining the condition

$$\lambda \leq \frac{r\widehat{\omega}_1}{\max_j \left| f'(u_{j+\frac{1}{2}}^\pm) \right|}, \text{ we conclude that } \bar{u}^* \geq 0.$$

Similarly, we obtain the formula for the cell average of u_j^{n+1} as follows:

$$\bar{u}_j^{n+1} = r \left(1 - \frac{r^2}{6K^2} \right) R_1 + \frac{r^2(4K^2 - r^2)}{24K^4} R_2 + \frac{r^2}{3K^2} R_3$$

where

$$R_3 = \left(\bar{u}_j^n - \lambda \widehat{H}_{j+\frac{1}{2}}^* + \lambda \widehat{H}_{j-\frac{1}{2}}^* \right)$$

According to the proof of positivity for (3.10), we also need to require $H^* = 0$ wherever $u^* = 0$ and the time step to satisfy the following constraint (notice that $\widehat{\omega}_1 = \widehat{\omega}_N$):

$$\frac{K^2}{r^2} \lambda^2 \max_j \beta_{j+\frac{1}{2}} \leq \widehat{\omega}_1.$$

Therefore, the whole PP time-step condition for the high order $S_2D_2O_4$ DG scheme using the fluxes (3.4), (3.6) and (3.8) in the one dimensional scalar conservation law is:

$$\lambda \max_j \left| f'(u_{j+\frac{1}{2}}^\pm) \right| \leq r\widehat{\omega}_1, \quad \lambda^2 \max_j \left\{ \alpha_{j+\frac{1}{2}}, \beta_{j+\frac{1}{2}} \right\} \leq \frac{r^2}{K^2} \widehat{\omega}_1. \quad (3.14)$$

Remark 1. Here and below, for the definition of $\alpha_{j+\frac{1}{2}}$ and $\beta_{j+\frac{1}{2}}$, in numerical implementation we replace $u_{j+\frac{1}{2}}^\pm = 0$ by $|u_{j+\frac{1}{2}}^\pm| < \epsilon_1$, and replace $u_{j+\frac{1}{2}}^\pm \neq 0$ by $|u_{j+\frac{1}{2}}^\pm| \geq \epsilon_1$, with $\epsilon_1 = 10^{-14}$.

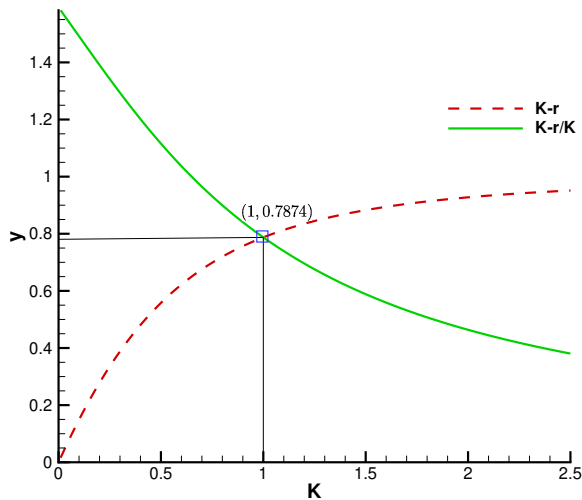


Figure 1: The curves of r versus K and $\frac{r}{K}$ versus K .

Remark 2. Based on Theorem 3.1, we draw the curves of r versus K and $\frac{r}{K}$ versus K in Figure 1. We can observe that r is increasing as K increases but $\frac{r}{K}$ is decreasing. Therefore, to obtain the optimal condition of (3.14), we take $K = 1$ and $r \approx 0.7874$.

Remark 3. Theorem 3.1 is a PP result rather than a bound-preserving result since (3.12) is only a positive linear combination rather than a convex combination. To have a bound-preserving result, we need (3.12) to be a convex combination, which is difficult to achieve.

Remark 4. In practice, the time step constraint may just be a sufficient condition for $\bar{u}^{n+1} \geq 0$. Also, it is hard to accurately estimate $\max_i \alpha_i$ and $\max_i \beta_i$. Besides, α_i and β_i might be very large numbers, leading to a very small time step condition in (3.14).

To alleviate such difficulties, in actual numerical computation, we will use the regular LF flux for \hat{H} and \hat{H}^* , and modify the flux to (3.6) and (3.8) only when some of the cell averages of the numerical solution at the next stage become less than zero. We can obtain a CFL condition in the $S_2D_2O_4$ DG scheme with the LF flux that satisfies L_2 stability by linear analysis. This linear analysis shows that the CFL number is 0.055. The specific algorithm is as follows:

- Step 1. Take $\Delta t = \frac{0.055}{\max_u |f'(u)|} \Delta x$, and take the fluxes \widehat{H} and \widehat{H}^* as:

$$\widehat{H}_{j+1/2} = \frac{1}{2} \left(H_{j+1/2}^- + H_{j+1/2}^+ - \alpha_{j+\frac{1}{2}} \left(u_{j+1/2}^+ - u_{j+1/2}^- \right) \right),$$

$$\widehat{H}_{j+1/2}^* = \frac{1}{2} \left(H_{j+1/2}^{*-} + H_{j+1/2}^{*+} - \beta_{j+\frac{1}{2}} \left(u_{j+1/2}^{*+} - u_{j+1/2}^{*-} \right) \right),$$

where

$$\alpha_{j+\frac{1}{2}} = \max_u |f'(u)|, \quad \beta_{j+\frac{1}{2}} = \max_u |f'(u)|$$

- Step 2. Change $\alpha_{j+\frac{1}{2}}, \beta_{j+\frac{1}{2}}$ by those given in (3.7) and (3.9) when $\bar{u}^* < 0$ for some cells, and keep the time step size unchanged. If the average of u^* is still less than zero, we rewind the computation back to the beginning of the current time step, and proceed with a halved time step. Otherwise, we calculate u^{n+1} using the same algorithmic process used to compute u^* . This step can be repeated if necessary. Theorem 3.1 guarantees that we need to rewind at most a fixed number of times.
- Step 3. Update the calculation time $t = t + \Delta t$, and restore the time step back to $\Delta t = \frac{0.055}{\max_u |f'(u)|} \Delta x$. Repeat the above calculations until the ending time T.

This algorithm is used in all the numerical experiments in Section 6.

3.2 The PP $S_2D_2O_4$ DG scheme for 2D scalar conservation laws in two dimensions

Consider the scalar conservation law in two space dimensions

$$u_t + f(u)_x + g(u)_y = 0. \tag{3.15}$$

Based on the equation, we can derive the expressions of u_t, u_{tt} as follows:

$$u_t = -f(u)_x - g(u)_y = -f'(u)u_x - g'(u)u_y$$

$$u_{tt} = -(f'(u)u_t)_x - (g'(u)u_t)_y = -(f''(u)u_x u_t + f'(u)u_{xt} + g''(u)u_y u_t + g'(u)u_{yt})$$

$$u_{xt} = -(f''(u)(u_x)^2 + f'(u)u_{xx} + g''(u)u_x u_y + g'(u)u_{xy})$$

$$u_{yt} = -(f''(u)u_y u_x + f'(u)u_{xy} + g''(u)(u_y)^2 + g'(u)u_{yy})$$

In the two dimensional space, we assume $\Omega = [a, b] \times [c, d]$ is discretized by $a = x_{\frac{1}{2}} < x_{\frac{3}{2}} < \dots < x_{N_x + \frac{1}{2}} = b$ and $c = y_{\frac{1}{2}} < y_{\frac{3}{2}} < \dots < y_{N_y + \frac{1}{2}} = d$ in the x and y directions, respectively. We denote by $K_{i,j} = I_i \times I_j = \left[x_{i-\frac{1}{2}}, x_{i+\frac{1}{2}} \right] \times \left[y_{j-\frac{1}{2}}, y_{j+\frac{1}{2}} \right]$ the cells in Ω for $i = 1, \dots, N_x, j = 1, \dots, N_y$, and by $\Delta x_i = x_{i+\frac{1}{2}} - x_{i-\frac{1}{2}}$ and $\Delta y_j = y_{j+\frac{1}{2}} - y_{j-\frac{1}{2}}$. We only consider the uniform meshes in this section, i.e. $\Delta x_i \equiv \Delta x$ and $\Delta y_j \equiv \Delta y$, for $i = 1, \dots, N_x, j = 1, \dots, N_y$. The finite element space in the DG scheme is taken as $W = \{v \in L^2 : v|_{K_{i,j}} \in P^3(K_{i,j}), i = 1, \dots, N_x, j = 1, \dots, N_y\}$, where $P^3(K)$ is the space of polynomials of degree ≤ 3 on each rectangle K . We denote $u_{i+\frac{1}{2},j}^\pm = u(x_{i+\frac{1}{2}}, y)|_{I_j}$, $u_{i,j+\frac{1}{2}}^\pm = u(x, y_{j+\frac{1}{2}})|_{I_i}$, $G_{i+\frac{1}{2},j}^\pm = u(x_{i+\frac{1}{2}}, y)|_{I_j}$ and $M_{i,j+\frac{1}{2}}^\pm = u(x, y_{j+\frac{1}{2}})|_{I_i}$. The quadrature rule adopted in two dimensional cells follows from tensor product and we denote $\hat{u}_{i,j}^{\eta,\delta} = u_{i,j}(\hat{x}_\eta, \hat{y}_\delta)$, $G_{i+\frac{1}{2},\delta}^\pm = u(x_{i+\frac{1}{2}}, \hat{y}_\delta)$, $M_{\eta,j+\frac{1}{2}}^\pm = u(\hat{x}_\eta, y_{j+\frac{1}{2}})$, $u_{i+\frac{1}{2},\delta}^\pm = u(x_{i+\frac{1}{2}}, \hat{y}_\delta)$ and $u_{\eta,j+\frac{1}{2}}^\pm = u(\hat{x}_\eta, y_{j+\frac{1}{2}})$, for $\eta, \delta = 1, \dots, 2N_q - 1$, on the cell $K_{i,j}$.

The $S_2D_2O_4$ DG scheme of the two dimensional conservation laws is based on the SSP $S_2D_2O_4$ time-stepping scheme in (2.1). For $M_1 = u_{i,j}^n + \frac{\Delta t}{r} F(u_{i,j}^n) = u_{i,j}^n - \frac{\Delta t}{r} [(f(u_{i,j}^n))_x + (g(u_{i,j}^n))_y]$, the DG scheme at the time level t^n is to find $M_1 \in W$, s.t. $\forall v_h \in W$,

$$\begin{aligned} \iint_{K_{ij}} M_1 v_h dx dy &= \iint_{K_{ij}} u_{i,j}^n v_h dx dy + \Delta t \left(\iint_{K_{ij}} f(x, y) (v_h)_x dx dy + \iint_{K_{ij}} g(x, y) (v_h)_y dx dy \right) \\ &- \Delta t \left(\int_{I_j} (\hat{f}_{i+\frac{1}{2},j}^{\text{LF}} v_{i+\frac{1}{2},j}^- - \hat{f}_{i-\frac{1}{2},j}^{\text{LF}} v_{i-\frac{1}{2},j}^+) dy + \int_{I_i} (\hat{g}_{i,j+\frac{1}{2}}^{\text{LF}} v_{i,j+\frac{1}{2}}^- - \hat{g}_{i,j-\frac{1}{2}}^{\text{LF}} v_{i,j-\frac{1}{2}}^+) dx \right) \end{aligned} \quad (3.16)$$

where \hat{f}^{LF} and \hat{g}^{LF} are the LF fluxes as used in [52].

For $M_2 = u_{i,j}^n + \frac{K^2}{r^2} \Delta t^2 \dot{F}(u_{i,j}^n) = u_{i,j}^n - \frac{K^2}{r^2} \Delta t^2 (G_x(u_{i,j}^n) + M_y(u_{i,j}^n))$ where $G = -f'(u)^2 u_x - f'(u)g'(u)u_y$, $M = -g'^2(u)u_y - f'(u)g'(u)u_x$, the DG scheme at the time level t^n is to find $M_2 \in W$, s.t. $\forall v_h \in W$,

$$\begin{aligned} \iint_{K_{ij}} M_2 v_h dx dy &= \iint_{K_{ij}} u_{i,j}^n v_h dx dy + \frac{K^2}{r^2} \Delta t \left(\iint_{K_{ij}} G(x, y) (v_h)_x dx dy + \iint_{K_{ij}} M(x, y) (v_h)_y dx dy \right) \\ &- \frac{K^2}{r^2} \Delta t \left(\int_{I_j} (\hat{G}_{i+\frac{1}{2},j} v_{i+\frac{1}{2},j}^- - \hat{G}_{i-\frac{1}{2},j} v_{i-\frac{1}{2},j}^+) dy + \int_{I_i} (\hat{M}_{i,j+\frac{1}{2}} v_{i,j+\frac{1}{2}}^- - \hat{M}_{i,j-\frac{1}{2}} v_{i,j-\frac{1}{2}}^+) dx \right) \end{aligned} \quad (3.17)$$

for $j = 1, 2, \dots, N$, where $\widehat{G}_{i+1/2,j}$ and $\widehat{M}_{i,j+1/2}$ are the numerical fluxes developed from the one dimension:

$$\widehat{G}_{i+1/2,j} = \frac{1}{2} \left(G_{i+1/2,j}^- + G_{i+1/2,j}^+ - \alpha_{i+1/2,j} \left(u_{i+1/2,j}^+ - u_{i+1/2,j}^- \right) \right), \quad (3.18)$$

$$\widehat{M}_{i,j+1/2} = \frac{1}{2} \left(M_{i,j+1/2}^- + M_{i,j+1/2}^+ - \alpha_{i,j+1/2} \left(u_{i,j+1/2}^+ - u_{i,j+1/2}^- \right) \right), \quad (3.19)$$

where the penalty parameter $\alpha_{i+1/2,j}$ is determined by ensuring the PP property for the scheme

(3.17):

$$\alpha_{i+1/2,j} = \begin{cases} \max \left\{ \left| \frac{G_{i+1/2,j}^+}{u_{i+1/2,j}^+} \right|, \left| \frac{G_{i+1/2,j}^-}{u_{i+1/2,j}^-} \right| \right\}, & \text{if } u_{i+1/2,j}^+ \neq 0 \text{ and } u_{i+1/2,j}^- \neq 0, \\ \left| \frac{G_{i+1/2,j}^+}{u_{i+1/2,j}^+} \right|, & \text{if } u_{i+1/2,j}^+ \neq 0 \text{ and } u_{i+1/2,j}^- = 0, \\ \left| \frac{G_{i+1/2,j}^-}{u_{i+1/2,j}^-} \right|, & \text{if } u_{i+1/2,j}^+ = 0 \text{ and } u_{i+1/2,j}^- \neq 0, \\ 0 & \text{if } u_{i+1/2,j}^+ = 0 \text{ and } u_{i+1/2,j}^- = 0. \end{cases} \quad (3.20)$$

Also, $\alpha_{i,j+1/2}$ has similar definition.

For $M_3 = u_{i,j}^* + \frac{K^2}{r^2} \Delta t^2 \dot{F}(u_{i,j}^*) = u_{i,j}^* - \frac{K^2}{r^2} \Delta t^2 (G_x^*(u_{i,j}^*) + M_y^*(u_{i,j}^*))$ where $G^* = -f'(u^*)^2 u_x^* - f'(u^*)g'(u^*)u_y^*$, $M^* = -g'^2(u^*)u_y^* - f'(u^*)g'(u^*)u_x^*$, the DG scheme is similar to (3.17), and the corresponding numerical flux $\widehat{G}_{i+1/2,j}^*$ and $\widehat{M}_{i,j+1/2}^*$ are defined as

$$\widehat{G}_{i+1/2,j}^* = \frac{1}{2} \left(G_{i+1/2,j}^{*-} + G_{i+1/2,j}^{*+} - \phi_{i+1/2,j} \left(u_{i+1/2,j}^{*+} - u_{i+1/2,j}^{*-} \right) \right), \quad (3.21)$$

$$\widehat{M}_{i,j+1/2}^* = \frac{1}{2} \left(M_{i,j+1/2}^{*-} + M_{i,j+1/2}^{*+} - \phi_{i,j+1/2} \left(u_{i,j+1/2}^{*+} - u_{i,j+1/2}^{*-} \right) \right), \quad (3.22)$$

with

$$\phi_{i+1/2,j} = \begin{cases} \max \left\{ \left| \frac{G_{i+1/2,j}^{*+}}{u_{i+1/2,j}^{*+}} \right|, \left| \frac{G_{i+1/2,j}^{*-}}{u_{i+1/2,j}^{*-}} \right| \right\}, & \text{if } u_{i+1/2,j}^{*+} \neq 0 \text{ and } u_{i+1/2,j}^{*-} \neq 0, \\ \left| \frac{G_{i+1/2,j}^{*+}}{u_{i+1/2,j}^{*+}} \right|, & \text{if } u_{i+1/2,j}^{*+} \neq 0 \text{ and } u_{i+1/2,j}^{*-} = 0, \\ \left| \frac{G_{i+1/2,j}^{*-}}{u_{i+1/2,j}^{*-}} \right|, & \text{if } u_{i+1/2,j}^{*+} = 0 \text{ and } u_{i+1/2,j}^{*-} \neq 0, \\ 0 & \text{if } u_{i+1/2,j}^{*+} = 0 \text{ and } u_{i+1/2,j}^{*-} = 0. \end{cases} \quad (3.23)$$

Also, $\phi_{i,j+1/2}$ has similar definition.

Theorem 3.2. For the fourth order $S_2D_2O_4$ DG scheme using the fluxes (3.18), (3.19), (3.21) and (3.22), if the following conditions are satisfied:

1. All point values at the Gauss-Lobatto quadrature points are non-negative: $\hat{u}_{i,j}^{\eta,\delta} \geq 0$.
2. For all i,j,η and δ , $G_{\eta,j\pm 1/2}^- = 0$ if $u_{\eta,j\pm 1/2}^- = 0$ and $G_{\eta,j\pm 1/2}^+ = 0$ if $u_{\eta,j\pm 1/2}^+ = 0$, $M_{i\pm 1/2,\delta}^- = 0$ if $u_{i\pm 1/2,\delta}^- = 0$, $M_{i\pm 1/2,\delta}^+ = 0$ if $u_{i\pm 1/2,\delta}^+ = 0$.

Then the cell average $\bar{u}_{i,j}^{n+1} \geq 0$ under the time step constraint below,

$$\begin{aligned} \frac{\Delta t}{\Delta x} \max_{i,j} |f'(u)| &\leq \frac{r}{2} \hat{\omega}_1, & \frac{\Delta t^2}{\Delta x^2} \max_{i,j} \left\{ \alpha_{i+\frac{1}{2},j}, \phi_{i+\frac{1}{2},j} \right\} &\leq \frac{r^2}{2K^2} \hat{\omega}_1 \\ \frac{\Delta t}{\Delta y} \max_{i,j} |g'(u)| &\leq \frac{r}{2} \hat{\omega}_1, & \frac{\Delta t^2}{\Delta y^2} \max_{i,j} \left\{ \alpha_{i,j+\frac{1}{2}}, \phi_{i,j+\frac{1}{2}} \right\} &\leq \frac{r^2}{2K^2} \hat{\omega}_1 \end{aligned}$$

Proof. Take the test function $v_h = 1$ on $K_{i,j}$ and zero anywhere else in the scheme (3.16) and (3.17) and denote $\lambda_x = \frac{\Delta t}{\Delta x}$, $\lambda_y = \frac{\Delta t}{\Delta y}$, we obtain the formula satisfied by the cell average of u^* in the cell $K_{i,j}$

$$\bar{u}_{i,j}^* = \left(1 - \frac{4rK^2 + r^2}{8K^2} \right) \bar{u}_{i,j}^n + \frac{r}{2} (\mathbf{R}_1 + \mathbf{R}_3) + \frac{r^2}{8K^2} (\mathbf{R}_2 + \mathbf{R}_4) \quad (3.24)$$

where

$$\begin{aligned} \mathbf{R}_1 &= \frac{1}{2} \bar{u}_{i,j}^n - \frac{\lambda_x}{r} \frac{1}{\Delta y} \int_{y_{j-\frac{1}{2}}}^{y_{j+\frac{1}{2}}} \hat{f}_{i+\frac{1}{2},j}^{\text{LF}} dy + \frac{\lambda_x}{r} \frac{1}{\Delta y} \int_{y_{j-\frac{1}{2}}}^{y_{j+\frac{1}{2}}} \hat{f}_{i-\frac{1}{2},j}^{\text{LF}} dy \\ \mathbf{R}_2 &= \frac{1}{2} \bar{u}_{i,j}^n - \frac{K^2}{r^2} \lambda_x^2 \frac{1}{\Delta y} \int_{y_{j-\frac{1}{2}}}^{y_{j+\frac{1}{2}}} \widehat{G}_{i+\frac{1}{2},j} dy + \frac{K^2}{r^2} \lambda_x^2 \frac{1}{\Delta y} \int_{y_{j-\frac{1}{2}}}^{y_{j+\frac{1}{2}}} \widehat{G}_{i-\frac{1}{2},j} dy \\ \mathbf{R}_3 &= \frac{1}{2} \bar{u}_{i,j}^n - \frac{\lambda_y}{r} \frac{1}{\Delta x} \int_{x_{i-\frac{1}{2}}}^{x_{i+\frac{1}{2}}} \hat{g}_{i,j+\frac{1}{2}}^{\text{LF}} dx + \frac{\lambda_y}{r} \frac{1}{\Delta x} \int_{x_{i-\frac{1}{2}}}^{x_{i+\frac{1}{2}}} \hat{g}_{i,j-\frac{1}{2}}^{\text{LF}} dx \\ \mathbf{R}_4 &= \frac{1}{2} \bar{u}_{i,j}^n - \frac{K^2}{r^2} \lambda_y^2 \frac{1}{\Delta x} \int_{x_{i-\frac{1}{2}}}^{x_{i+\frac{1}{2}}} \widehat{M}_{i,j+\frac{1}{2}} dx + \frac{K^2}{r^2} \lambda_y^2 \frac{1}{\Delta x} \int_{x_{i-\frac{1}{2}}}^{x_{i+\frac{1}{2}}} \widehat{M}_{i,j-\frac{1}{2}} dx \end{aligned}$$

and the average of u_{ij}^n is

$$\begin{aligned} \bar{u}_{ij}^n &= \frac{1}{\Delta x \Delta y} \int_{x_{i-1/2}}^{x_{i+1/2}} \int_{y_{j-1/2}}^{y_{j+1/2}} u_{ij}(x, y) dx dy \\ &= \sum_{\eta=1}^{2N_q-1} \sum_{\delta=1}^{2N_q-1} \widehat{\omega}_\eta \widehat{\omega}_\delta u_{ij}(\hat{x}_i^\eta, \hat{y}_j^\delta) \end{aligned} \quad (3.25)$$

Since R_1 and R_3 has exactly the same form as in [52], we have $R_1 \geq 0$ and $R_3 \geq 0$, under the condition $\lambda_x \leq \frac{r\hat{\omega}_1}{2 \max_j |f'(u_{j+\frac{1}{2}}^\pm)|}$, $\lambda_y \leq \frac{r\hat{\omega}_1}{2 \max_j |g'(u_{j+\frac{1}{2}}^\pm)|}$. For R_2 , we substitute the expression of (3.25) and (3.18) and obtain

$$\begin{aligned}
R_2 &= \frac{1}{2} \sum_{\delta=1}^{2N_q-1} \sum_{\eta=2}^{2N_q-2} \hat{w}_\eta \hat{w}_\delta u_{ij} (\hat{x}_i^\eta, \hat{y}_j^\delta) \\
&+ \sum_{\delta=1}^{2N_q-1} \hat{w}_\delta \left[\frac{1}{2} \hat{w}_1 - \frac{K^2}{2r^2} \lambda_x^2 \left(\frac{G_{i+\frac{1}{2},\delta}^-}{u_{i+\frac{1}{2},\delta}^-} + \alpha_{i+\frac{1}{2},\delta} \right) \right] u_{i+\frac{1}{2},\delta}^- \\
&+ \sum_{\delta=1}^{2N_q-1} \hat{w}_\delta \left[\frac{1}{2} \hat{w}_1 - \frac{K^2}{2r^2} \lambda_x^2 \left(\alpha_{i-\frac{1}{2},\delta} - \frac{G_{i-\frac{1}{2},\delta}^+}{u_{i-\frac{1}{2},\delta}^+} \right) \right] u_{i-\frac{1}{2},\delta}^+ \\
&+ \frac{K^2}{2r^2} \lambda_x^2 \sum_{\delta=1}^{2N_q-1} \hat{w}_\delta \left[\frac{G_{i-\frac{1}{2},\delta}^-}{u_{i-\frac{1}{2},\delta}^-} + \alpha_{i-\frac{1}{2},\delta} \right] u_{i-\frac{1}{2},\delta}^- + \frac{K^2}{2r^2} \lambda_x^2 \sum_{\delta=1}^{2N_q-1} \hat{w}_\delta \left[\alpha_{i+\frac{1}{2},\delta} - \frac{G_{i+\frac{1}{2},\delta}^+}{u_{i+\frac{1}{2},\delta}^+} \right] u_{i+\frac{1}{2},\delta}^+
\end{aligned} \tag{3.26}$$

To satisfy a positive linear combination of point values $u_{i\pm\frac{1}{2},\delta}^\pm$ and $u_{ij}(\hat{x}_i^\eta, \hat{y}_j^\delta)$ of the right hand side in (3.26), it suffices to require $G = 0$ if $u = 0$ and the time step to satisfy the following constraint:

$$\frac{K^2}{r^2} \max_{i,j} \left\{ \alpha_{i+\frac{1}{2},j} + \frac{G_{i+\frac{1}{2},j}^-}{u_{i+\frac{1}{2},j}^-}, \alpha_{i-\frac{1}{2},j} - \frac{G_{i-\frac{1}{2},j}^+}{u_{i-\frac{1}{2},j}^+} \right\} \lambda_x^2 \leq \hat{\omega}_1.$$

We have similar conclusion that we should require $M = 0$ wherever $u = 0$ and have the following time-step condition

$$\frac{K^2}{r^2} \max_{i,j} \left\{ \alpha_{i,j+\frac{1}{2}} + \frac{M_{i,j+\frac{1}{2}}^-}{u_{i,j+\frac{1}{2}}^-}, \alpha_{i,j-\frac{1}{2}} - \frac{M_{i,j-\frac{1}{2}}^+}{u_{i,j-\frac{1}{2}}^+} \right\} \lambda_y^2 \leq \hat{\omega}_1.$$

According to the definition of $\alpha_{i+\frac{1}{2},j}$ and $\alpha_{i,j+\frac{1}{2}}$ in (3.20), the condition on the time step above can be further simplified as the following time-step condition:

$$\begin{aligned}
\frac{2K^2}{r^2} \lambda_x^2 \max_{i,j} \alpha_{i+\frac{1}{2},j} &\leq \hat{\omega}_1, \\
\frac{2K^2}{r^2} \lambda_y^2 \max_{i,j} \alpha_{i,j+\frac{1}{2}} &\leq \hat{\omega}_1.
\end{aligned}$$

Similarly, we obtain the formula satisfied by the cell average of u^{n+1} in the cell $K_{i,j}$

$$\bar{u}_j^{n+1} = r \left(1 - \frac{r^2}{6K^2} \right) (R_1 + R_3) + \frac{r^2 (4K^2 - r^2)}{24K^4} (R_2 + R_4) + \frac{r^2}{3K^2} (R_5 + R_6)$$

where

$$\begin{aligned} R_5 &= \frac{1}{2}\bar{u}_{i,j}^* - \frac{K^2}{r^2}\lambda_x^2 \frac{1}{\Delta y} \int_{y_{j-\frac{1}{2}}}^{y_{j+\frac{1}{2}}} \widehat{G}_{i+\frac{1}{2},j}^* dy + \frac{K^2}{r^2}\lambda_x^2 \frac{1}{\Delta y} \int_{y_{j-\frac{1}{2}}}^{y_{j+\frac{1}{2}}} \widehat{G}_{i-\frac{1}{2},j}^* dy \\ R_6 &= \frac{1}{2}\bar{u}_{i,j}^* - \frac{K^2}{r^2}\lambda_y^2 \frac{1}{\Delta x} \int_{x_{i-\frac{1}{2}}}^{x_{i+\frac{1}{2}}} \widehat{M}_{i,j+\frac{1}{2}}^* dx + \frac{K^2}{r^2}\lambda_y^2 \frac{1}{\Delta x} \int_{x_{i-\frac{1}{2}}}^{x_{i+\frac{1}{2}}} \widehat{M}_{i,j-\frac{1}{2}}^* dx \end{aligned}$$

Similar to the proof of the PP property in (3.24), it suffices to require $G^* = 0$ and $M^* = 0$ wherever $u^* = 0$ and the time step to satisfy the following constraint:

$$\begin{aligned} \frac{2K^2}{r^2}\lambda_x^2 \max_{i,j} \left\{ \phi_{i+\frac{1}{2},j} \right\} &\leq \widehat{\omega}_1, \\ \frac{2K^2}{r^2}\lambda_y^2 \max_{i,j} \left\{ \phi_{i,j+\frac{1}{2}} \right\} &\leq \widehat{\omega}_1. \end{aligned}$$

Therefore, the whole PP time step condition for $\bar{u}_{i,j}^{n+1} \geq 0$ is:

$$\begin{aligned} \frac{\Delta t}{\Delta x} \max |f'(u)| &\leq \frac{r}{2}\widehat{\omega}_1, \quad \frac{\Delta t^2}{\Delta x^2} \max_{i,j} \left\{ \alpha_{i+\frac{1}{2},j}, \phi_{i+\frac{1}{2},j} \right\} \leq \frac{r^2}{2K^2}\widehat{\omega}_1 \\ \frac{\Delta t}{\Delta y} \max |g'(u)| &\leq \frac{r}{2}\widehat{\omega}_1, \quad \frac{\Delta t^2}{\Delta y^2} \max_{i,j} \left\{ \alpha_{i,j+\frac{1}{2}}, \phi_{j+\frac{1}{2}} \right\} \leq \frac{r^2}{2K^2}\widehat{\omega}_1 \end{aligned}$$

4 The PP $S_2D_2O_4$ DG scheme for the Euler equations

4.1 The PP $S_2D_2O_4$ DG scheme for the compressible Euler equations in one dimension

Consider the one-dimensional compressible Euler equations (4.1).

$$\mathbf{U}_t + \mathbf{f}(\mathbf{U})_x = \mathbf{0}, \quad x \in \mathbb{R}, t > 0 \quad (4.1)$$

where

$$\mathbf{U} = \begin{pmatrix} \rho \\ m \\ E \end{pmatrix}, \quad \mathbf{f}(\mathbf{U}) = \begin{pmatrix} m \\ \rho u^2 + p \\ (E + p)u \end{pmatrix}$$

with

$$m = \rho u, \quad E = \frac{1}{2}\rho u^2 + \rho e$$

in which ρ is the density of fluid, m is the momentum, u is the velocity, E is the total energy, p is the pressure and for the ideal gas $p = (\gamma - 1)\rho e$, e is the specific internal energy, and $\gamma > 1$ is the ratio of specific heats. It is well-known that the physical solution $\mathbf{U} \in G$ for all $t > 0$ if it holds at $t = 0$, where G is the admissible set of solutions defined as

$$G = \{\mathbf{U} : \rho \geq 0, p(\mathbf{U}) \geq 0\}.$$

Take $\hat{\gamma} = \gamma - 1$, then direct computation gives the expressions of \mathbf{U}_t and \mathbf{U}_{tt} as follows:

$$\begin{aligned} u &= \frac{m}{\rho} \\ u_x &= \frac{m_x}{\rho} - \frac{u\rho_x}{\rho} \\ \rho_t &= -m_x, \\ m_t &= -(\rho u^2 + p)_x = -\left(\hat{\gamma}E_x + \frac{3-\gamma}{2}m_x u + \frac{3-\gamma}{2}m u_x\right) \\ E_t &= -[(E + p)u]_x = -\left(\gamma E_x u + \gamma E u_x - \frac{\hat{\gamma}}{2}m_x u^2 - \hat{\gamma}m u u_x\right) \\ u_t &= \frac{m_t}{\rho} - \frac{u\rho_t}{\rho}, \\ \rho_{tt} &= -m_{tx} = -\left(\hat{\gamma}E_x + \frac{3-\gamma}{2}m_x u + \frac{3-\gamma}{2}m u_x\right)_x := -A_x \\ m_{tt} &= -\left(\hat{\gamma}E_t + \frac{3-\gamma}{2}m_t u + \frac{3-\gamma}{2}m u_t\right)_x := -B_x \\ E_{tt} &= -\left(\gamma E_t u + \gamma E u_t - \frac{\hat{\gamma}}{2}m_t u^2 - \hat{\gamma}m u u_t\right)_x := -C_x \end{aligned}$$

The one dimensional $S_2D_2O_4$ DG scheme for the compressible Euler equations is constructed according to the scheme (2.1). For $M_1 = \mathbf{U}_j^n + \frac{\Delta t}{r} F(\mathbf{U}_j^n) = \mathbf{U}_j^n - \frac{\Delta t}{r} \mathbf{f}(\mathbf{U}_j^n)_x$, the DG scheme at time level t^n is to find $M_1 \in V$, s.t. $\forall v_h \in V$,

$$\int_{I_j} M_1 v_h dx = \int_{I_j} \mathbf{U}_j^n v_h dx + \Delta t \left(\int_{I_j} \mathbf{f}(\mathbf{U}_j^n, \Delta t) (v_h)_x dx - \hat{\mathbf{f}}_{j+\frac{1}{2}}^{\text{LF}} (v_h)_{j+\frac{1}{2}}^- + \hat{\mathbf{f}}_{j-\frac{1}{2}}^{\text{LF}} (v_h)_{j-\frac{1}{2}}^+ \right) \quad (4.2)$$

holds for $j = 1, 2, \dots, N$, where $\hat{\mathbf{f}}^{\text{LF}}$ is the LF flux used in the DG schemes for the Euler equations in [51].

For $M_2 = \mathbf{U}_j^n + \frac{K^2}{r^2} \Delta t^2 \dot{F}(\mathbf{U}_j^n) = \mathbf{U}_j^n - \frac{K^2}{r^2} \Delta t^2 \mathbf{H}_x$ where $\mathbf{H}_x = \begin{pmatrix} A_x \\ B_x \\ C_x \end{pmatrix}$, the DG scheme

at time level t^n is to find $M_2 \in V$, s.t. $\forall v_h \in V$,

$$\int_{I_j} M_2 v_h dx = \int_{I_j} \mathbf{U}_j^n v_h dx + \Delta t \left(\int_{I_j} \mathbf{H}(x) (v_h)_x dx - \widehat{\mathbf{H}}_{j+\frac{1}{2}} (v_h)_{j+\frac{1}{2}}^- + \widehat{\mathbf{H}}_{j-\frac{1}{2}} (v_h)_{j-\frac{1}{2}}^+ \right) \quad (4.3)$$

for $j = 1, 2, \dots, N$. $\widehat{\mathbf{H}}_{j+\frac{1}{2}}$ is the numerical flux at $x_{j+\frac{1}{2}}$ defined as

$$\widehat{\mathbf{H}}_{j+1/2} = \frac{1}{2} \left(\mathbf{H}_{j+1/2}^- + \mathbf{H}_{j+1/2}^+ - \alpha_{j+\frac{1}{2}} \left(\mathbf{U}_{j+1/2}^+ - \mathbf{U}_{j+1/2}^- \right) \right) \quad (4.4)$$

where the penalty parameter $\alpha_{j+\frac{1}{2}}$ is defined as (4.9) for the propose of PP property.

For $M_3 = \mathbf{U}_j^* + \frac{K^2}{r^2} \Delta t^2 \dot{F}(\mathbf{U}_j^*) = \mathbf{U}_j^* - \frac{K^2}{r^2} \Delta t^2 \mathbf{H}(\mathbf{U}_j^*)_x$, the DG scheme is similar to (4.3), and the numerical flux $\widehat{\mathbf{H}}_{j+\frac{1}{2}}^*$ at $x_{j+\frac{1}{2}}$ is defined as

$$\widehat{\mathbf{H}}_{j+1/2}^* = \frac{1}{2} \left(\mathbf{H}_{j+1/2}^{*-} + \mathbf{H}_{j+1/2}^{*+} - \beta_{j+\frac{1}{2}} \left(\mathbf{U}_{j+1/2}^{*+} - \mathbf{U}_{j+1/2}^{*-} \right) \right) \quad (4.5)$$

where $\beta_{j+\frac{1}{2}}$ has the similar definition as $\alpha_{j+\frac{1}{2}}$.

Theorem 4.1. *For the fourth order $S_2D_2O_4$ DG scheme of the one dimensional compressible Euler equations using the fluxes (4.4) and (4.5), given $\mathbf{U}^n \in G$, then the cell average $\bar{\mathbf{U}}^{n+1} \in G$ under the time step constraint below,*

$$\frac{\Delta t}{\Delta x} \max_j \| |u| + c \|_\infty \leq r \widehat{\omega}_1, \quad \frac{\Delta t^2}{\Delta x^2} \max_j \left\{ \alpha_{j+\frac{1}{2}}, \beta_{j+\frac{1}{2}} \right\} \leq \frac{r^2}{K^2} \widehat{\omega}_1, \quad \text{where } c = \sqrt{\frac{\gamma p}{\rho}}$$

Proof. Take the test function $v_h = 1$ on I_j and zero anywhere else in the scheme (4.2) and (4.3) and denote $\lambda = \frac{\Delta t}{\Delta x}$, we obtain the equation satisfied by the cell average of \mathbf{U}^* in I_j ,

$$\bar{\mathbf{U}}_j^* = \left(1 - \frac{4rK^2 + r^2}{8K^2} \right) \bar{\mathbf{U}}_j^n + \frac{r}{2} \mathbf{R}_1 + \frac{r^2}{8K^2} \mathbf{R}_2, \quad (4.6)$$

where

$$\begin{aligned} \mathbf{R}_1 &= \left(\bar{\mathbf{U}}_j^n - \frac{\lambda}{r} \widehat{\mathbf{f}}_{j+\frac{1}{2}}^{\text{LF}} + \frac{\lambda}{r} \widehat{\mathbf{f}}_{j-\frac{1}{2}}^{\text{LF}} \right) \\ \mathbf{R}_2 &= \left(\bar{\mathbf{U}}_j^n - \frac{K^2}{r^2} \lambda^2 \widehat{\mathbf{H}}_{j+\frac{1}{2}} + \frac{K^2}{r^2} \lambda^2 \widehat{\mathbf{H}}_{j-\frac{1}{2}} \right) \end{aligned}$$

and the average is

$$\bar{\mathbf{U}}_j^n = \sum_{\mu=1}^{2N_q-1} \widehat{\omega}_\mu \mathbf{U}_j(\hat{x}_j^\mu) \quad (4.7)$$

Since R_1 has exactly the same form as in [51], $R_1 \in G$ is guaranteed under the condition $\lambda \leq \frac{r\hat{w}_1}{\max_j \| |u|+c \|_\infty}$. Next we further rewrite R_2 by (4.4) and (4.7),

$$\begin{aligned}
R_2 = & \left(\hat{w}_1 - \frac{K^2}{2r^2} \lambda^2 \alpha_{j-\frac{1}{2}} \right) \left(\mathbf{U}_{j-\frac{1}{2}}^+ + \frac{K^2}{2r^2} \lambda^2 \left(\hat{w}_1 - \frac{K^2}{2r^2} \lambda^2 \alpha_{j-\frac{1}{2}} \right)^{-1} \mathbf{H} \left(\mathbf{U}_{j-\frac{1}{2}}^+ \right) \right) \\
& + \left(\hat{w}_{2N_q-1} - \frac{K^2}{2r^2} \lambda^2 \alpha_{j+\frac{1}{2}} \right) \left(\mathbf{U}_{j+\frac{1}{2}}^- - \frac{K^2}{2r^2} \lambda^2 \left(\hat{w}_{2N_q-1} - \frac{K^2}{2r^2} \lambda^2 \alpha_{j+\frac{1}{2}} \right)^{-1} \mathbf{H} \left(\mathbf{U}_{j+\frac{1}{2}}^- \right) \right) \\
& + \frac{K^2}{2r^2} \lambda^2 \alpha_{j-\frac{1}{2}} \left(\mathbf{U}_{j-\frac{1}{2}}^- + \alpha_{j-\frac{1}{2}}^{-1} \mathbf{H} \left(\mathbf{U}_{j-\frac{1}{2}}^- \right) \right) \\
& + \frac{K^2}{2r^2} \lambda^2 \alpha_{j+\frac{1}{2}} \left(\mathbf{U}_{j+\frac{1}{2}}^+ - \alpha_{j+\frac{1}{2}}^{-1} \mathbf{H} \left(\mathbf{U}_{j+\frac{1}{2}}^+ \right) \right) \\
& + \sum_{\mu=2}^{2N_q-2} \hat{w}_\mu \mathbf{U}_j \left(\hat{x}_j^\mu \right)
\end{aligned}$$

The last term is automatically in the admissible set G , since the weights $\hat{w}_\mu \geq 0$ and the nodal values $\mathbf{U}_j \left(\hat{x}_j^\mu \right) \in G$. The PP property of the remaining terms is guaranteed by our choice of α , which is launched based on the idea of Zhang [49]. Next we want to obtain $\mathbf{U}_{j-\frac{1}{2}}^- + \alpha_{j-\frac{1}{2}}^{-1} \mathbf{H} \left(\mathbf{U}_{j-\frac{1}{2}}^- \right) \in G$. We define the function

$$\chi(\mathbf{U}) = \rho E - \frac{1}{2} \|\rho \mathbf{U}\|^2$$

Thus a vector $\mathbf{U} \in G$ if and only if its first component and $\chi(\mathbf{U})$ are positive. First we have

$$\begin{aligned}
\alpha \mathbf{U} \pm \mathbf{H}(\mathbf{U}) &= (\alpha \pm v) \begin{pmatrix} \rho \\ \rho u \\ E \end{pmatrix} \pm \begin{pmatrix} 0 \\ M \\ N \end{pmatrix} \\
&= \begin{pmatrix} \bar{\alpha} \rho \\ \bar{\alpha} \rho u \pm M \\ \bar{\alpha} E \pm N \end{pmatrix}
\end{aligned}$$

where

$$v = \frac{A}{\rho}, \quad M = B - Au, \quad N = C - \frac{E}{\rho} A$$

with $v = \frac{A}{\rho}$ and $\bar{\alpha}$ denotes $\alpha \pm v$. Then we get

$$\begin{aligned}
& \chi(\alpha \mathbf{U} \pm \mathbf{H}(\mathbf{U})) \\
&= \bar{\alpha}^2 \rho E \pm \bar{\alpha} \rho N - \frac{1}{2}(\bar{\alpha} \rho u \pm M)^2 \\
&= \bar{\alpha}^2 \rho \left(E - \frac{1}{2} \rho u^2 \right) \pm \bar{\alpha} \rho (N - uM) - \frac{1}{2} M^2 \\
&= \rho^2 e \bar{\alpha}^2 \pm \rho (N - uM) \bar{\alpha} - \frac{1}{2} M^2
\end{aligned} \tag{4.8}$$

Therefore, if the following condition on α is satisfied:

$$\alpha_{j+\frac{1}{2}} \geq \max_{\mathbf{U}_{j+\frac{1}{2}}^-, \mathbf{U}_{j+\frac{1}{2}}^+} \left[|v| + \frac{1}{2\rho^2 e} \left(\sqrt{\rho^2 (N - uM)^2 + 2M^2 \rho^2 e} + \rho |N - uM| \right) \right], \tag{4.9}$$

then we have $\chi(\alpha \mathbf{U} \pm \mathbf{H}(\mathbf{U})) \geq 0$. We will take equality in (4.9) for choosing α .

We note that $\frac{K^2}{r^2} \lambda^2 \alpha \leq \hat{\omega}_1$ if and only if $0 \leq \frac{K^2}{2r^2} \lambda^2 \left(\hat{\omega}_1 - \frac{K^2}{2r^2} \lambda^2 \alpha \right)^{-1} \leq \alpha^{-1}$. Therefore, when λ satisfies $\frac{K^2}{r^2} \lambda^2 \max_j \alpha_{j+\frac{1}{2}} \leq \hat{\omega}_1$, we have

$$\begin{aligned}
\mathbf{U}_{j-\frac{1}{2}}^-, \mathbf{U}_{j+\frac{1}{2}}^+ \in G &\Rightarrow \mathbf{U}_{j-\frac{1}{2}}^- + \alpha_{j-\frac{1}{2}}^{-1} \mathbf{H} \left(\mathbf{U}_{j-\frac{1}{2}}^- \right) \in G, \mathbf{U}_{j+\frac{1}{2}}^+ - \alpha_{j+\frac{1}{2}}^{-1} \mathbf{H} \left(\mathbf{U}_{j+\frac{1}{2}}^+ \right) \in G \\
\mathbf{U}_{j-\frac{1}{2}}^+ \in G &\Rightarrow \mathbf{U}_{j-\frac{1}{2}}^+ + \frac{K^2}{2r^2} \lambda^2 \left(\hat{\omega}_1 - \frac{K^2}{2r^2} \lambda^2 \alpha_{j-\frac{1}{2}} \right)^{-1} \mathbf{H} \left(\mathbf{U}_{j-\frac{1}{2}}^+ \right) \in G \\
\mathbf{U}_{j+\frac{1}{2}}^- \in G &\Rightarrow \mathbf{U}_{j+\frac{1}{2}}^- - \frac{K^2}{2r^2} \lambda^2 \left(\hat{\omega}_{2N_q-1} - \frac{K^2}{2r^2} \lambda^2 \alpha_{j+\frac{1}{2}} \right)^{-1} \mathbf{H} \left(\mathbf{U}_{j+\frac{1}{2}}^- \right) \in G
\end{aligned}$$

Then under the condition:

$$\begin{aligned}
\lambda &\leq \frac{r \hat{\omega}_1}{\max_j \| |u| + c \|_\infty} \\
\frac{K^2}{r^2} \lambda^2 \max_j \alpha_{j+\frac{1}{2}} &\leq \hat{\omega}_1
\end{aligned}$$

we have $\bar{\mathbf{U}}^* \in G$.

Similarly, we obtain the equation satisfied by the cell average of \mathbf{U}^{n+1} on cell I_j

$$\bar{\mathbf{U}}_j^{n+1} = r \left(1 - \frac{r^2}{6K^2} \right) \mathbf{R}_1 + \frac{r^2 (4K^2 - r^2)}{24K^4} \mathbf{R}_2 + \frac{r^2}{3K^2} \mathbf{R}_3$$

where

$$\mathbf{R}_3 = \left(\bar{\mathbf{U}}_j^* - \frac{K^2}{r^2} \lambda^2 \hat{\mathbf{H}}_{j+\frac{1}{2}}^* + \frac{K^2}{r^2} \lambda^2 \hat{\mathbf{H}}_{j-\frac{1}{2}}^* \right)$$

and $\beta_{j+\frac{1}{2}}$ has the similar definition as $\alpha_{j+\frac{1}{2}}$. Therefore, we have the similar PP conclusion as (4.6).

4.2 The PP $S_2D_2O_4$ DG scheme for the compressible Euler equations in two dimensions

Consider the compressible Euler equations (4.10) of gas dynamics in two space dimensions

$$\mathbf{U}_t + \mathbf{f}(\mathbf{U})_x + \mathbf{g}(\mathbf{U})_y = \mathbf{0}, \quad (4.10)$$

where

$$\mathbf{U} = \begin{pmatrix} \rho \\ m \\ n \\ E \end{pmatrix}, \quad \mathbf{f}(\mathbf{U}) = \begin{pmatrix} \rho u \\ \rho u^2 + p \\ \rho uv \\ (E + p)u \end{pmatrix}, \quad \mathbf{g}(\mathbf{U}) = \begin{pmatrix} \rho v \\ \rho uv \\ \rho v^2 + p \\ (E + p)v \end{pmatrix},$$

$$m = \rho u, \quad n = \rho v, \quad E = \frac{1}{2}\rho u^2 + \frac{1}{2}\rho v^2 + \rho e, \quad p = (\gamma - 1)\rho e.$$

We define the set of admissible states as

$$G = \left\{ \mathbf{U} = \begin{pmatrix} \rho \\ \rho u \\ \rho v \\ E \end{pmatrix} : \rho > 0, \quad \rho e(\mathbf{U}) = E - \frac{1}{2}\rho(u^2 + v^2) > 0 \right\}.$$

Take $\hat{\gamma} = \gamma - 1$, then the expressions of \mathbf{U}_t and \mathbf{U}_{tt} are as follows:

$$u = \frac{m}{\rho}$$

$$v = \frac{n}{\rho}$$

$$u_x = \frac{m_x}{\rho} - \frac{u\rho_x}{\rho}$$

$$u_y = \frac{m_y}{\rho} - \frac{u\rho_y}{\rho}$$

$$v_x = \frac{n_x}{\rho} - \frac{v\rho_x}{\rho},$$

$$v_y = \frac{n_y}{\rho} - \frac{v\rho_y}{\rho}$$

$$\rho_t = -m_x - n_y$$

$$m_t = - \left(\hat{\gamma} E_x + \frac{3-\gamma}{2} m_x u + \frac{3-\gamma}{2} m u_x - \frac{\hat{\gamma}}{2} n_x v - \frac{\hat{\gamma}}{2} n v_x + m_y v + m v_y \right),$$

$$n_t = - \left(n_x u + n u_x + \hat{\gamma} E_y - \frac{\hat{\gamma}}{2} m_y u - \frac{\hat{\gamma}}{2} m u_y + \frac{3-\gamma}{2} n_y v + \frac{3-\gamma}{2} n v_y \right),$$

$$E_t = - \left(\gamma E_x u + \gamma E u_x - \frac{\hat{\gamma}}{2} m_x u^2 - \hat{\gamma} m u u_x - \frac{\hat{\gamma}}{2} m_x v^2 - \hat{\gamma} m v v_x \right)$$

$$- \left(\gamma E_y v + \gamma E v_y - \frac{\hat{\gamma}}{2} n_y u^2 - \hat{\gamma} n u u_y - \frac{\hat{\gamma}}{2} n_y v^2 - \hat{\gamma} n v v_y \right)$$

$$u_t = \frac{m_t}{\rho} - \frac{u\rho_t}{\rho}$$

$$v_t = \frac{n_t}{\rho} - \frac{v\rho_t}{\rho}$$

$$\rho_{tt} = -m_{tx} - n_{ty} := -A_x - J_y,$$

$$m_{tt} = - \left(\hat{\gamma} E_t + \frac{3-\gamma}{2} m_t u + \frac{3-\gamma}{2} m u_t - \frac{\hat{\gamma}}{2} n_t v - \frac{\hat{\gamma}}{2} n v_t \right)_x - (m_t v + m v_t)_y$$

$$:= -B_x - K_y$$

$$n_{tt} = - (n u_t + n_t u)_x - \left(\hat{\gamma} E_t - \frac{\hat{\gamma}}{2} m_t u - \frac{\hat{\gamma}}{2} m u_t + \frac{3-\gamma}{2} n_t v + \frac{3-\gamma}{2} n v_t \right)_y$$

$$:= -C_x - L_y$$

$$E_{tt} = - \left(\gamma E_t u + \gamma E u_t - \frac{\hat{\gamma}}{2} m_t u^2 - 2\hat{\gamma} m u u_t - \frac{\hat{\gamma}}{2} m_t v^2 - 2\hat{\gamma} m v v_t \right)_x$$

$$- \left(\gamma E_t v + \gamma E v_t - \frac{\hat{\gamma}}{2} n_t u^2 - 2\hat{\gamma} n u u_t - \frac{\hat{\gamma}}{2} n_t v^2 - 2\hat{\gamma} n v v_t \right)_y$$

$$:= -D_x - M_y$$

We design the $S_2D_2O_4$ DG scheme for the two-dimensional compressible Euler equations based on the scheme in (2.1). For $M_1 = \mathbf{U}_{i,j}^n + \frac{\Delta t}{r} F(\mathbf{U}_{i,j}^n) = \mathbf{U}_j^n - \frac{\Delta t}{r} f(\mathbf{U}_{i,j}^n)_x - g(\mathbf{U}_{i,j}^n)_y$, the $S_2D_2O_4$ DG scheme at time level t^n is to find $M_1 \in V$, s.t. $\forall v_h \in V$,

$$\begin{aligned} \iint_{K_{ij}} M_1 v_h dx dy &= \iint_{K_{ij}} \mathbf{U}_{i,j}^n v_h dx dy + \frac{\Delta t}{r} \left(\iint_{K_{ij}} \mathbf{f}(\mathbf{U}_{i,j}^n) (v_h)_x dx dy + \iint_{K_{ij}} \mathbf{g}(\mathbf{U}_{i,j}^n) (v_h)_y dx dy \right) \\ &- \frac{\Delta t}{r} \left(\int_{I_j} (\hat{\mathbf{f}}_{i+\frac{1}{2},j}^{\text{LF}} v_{i+\frac{1}{2},j}^- - \hat{\mathbf{f}}_{i-\frac{1}{2},j}^{\text{LF}} v_{i-\frac{1}{2},j}^+) dy + \int_{I_j} (\hat{\mathbf{g}}_{i,j+\frac{1}{2}}^{\text{LF}} v_{i,j+\frac{1}{2}}^- - \hat{\mathbf{g}}_{i,j-\frac{1}{2}}^{\text{LF}} v_{i,j-\frac{1}{2}}^+) dx \right) \end{aligned} \quad (4.11)$$

where $\hat{\mathbf{f}}^{\text{LF}}$ and $\hat{\mathbf{g}}^{\text{LF}}$ are the LF flux for the Euler equations in [51].

For $M_2 = \mathbf{U}_{i,j}^n + \frac{K^2}{r^2} \Delta t^2 \dot{F}(\mathbf{U}_{i,j}^n) = \mathbf{U}_{i,j}^n - \frac{K^2}{r^2} \Delta t^2 (\mathbf{H}_x + \mathbf{G}_y)$ where

$$\mathbf{H}_x = \begin{pmatrix} A_x \\ B_x \\ C_x \\ D_x \end{pmatrix}, \quad \mathbf{G}_y = \begin{pmatrix} J_y \\ K_y \\ L_y \\ M_y \end{pmatrix}$$

the DG scheme at time level t^n is to find $M_2 \in W$, s.t. $\forall v_h \in W$,

$$\begin{aligned} \iint_{K_{ij}} M_2 v_h dx dy &= \iint_{K_{ij}} \mathbf{U}_{i,j}^n v_h dx dy + \Delta t \left(\iint_{K_{ij}} \mathbf{H}(x,y) (v_h)_x dx dy + \iint_{K_{ij}} \mathbf{G}(x,y) (v_h)_y dx dy \right) \\ &- \Delta t \left(\int_{I_j} (\hat{\mathbf{H}}_{i+\frac{1}{2},j} v_{i+\frac{1}{2},j}^- - \hat{\mathbf{H}}_{i-\frac{1}{2},j} v_{i-\frac{1}{2},j}^+) dy + \int_{I_j} (\hat{\mathbf{G}}_{i,j+\frac{1}{2}} v_{i,j+\frac{1}{2}}^- - \hat{\mathbf{G}}_{i,j-\frac{1}{2}} v_{i,j-\frac{1}{2}}^+) dx \right) \end{aligned} \quad (4.12)$$

the corresponding numerical fluxes $\hat{\mathbf{H}}_{i+\frac{1}{2},j}$, $\hat{\mathbf{G}}_{i,j+\frac{1}{2}}$ are defined as

$$\hat{\mathbf{H}}_{i+1/2,j} = \frac{1}{2} \left(\mathbf{H}_{i+1/2,j}^- + \mathbf{H}_{i+1/2,j}^+ - \alpha_{i+\frac{1}{2},j} \left(\mathbf{U}_{i+1/2,j}^+ - \mathbf{U}_{i+1/2,j}^- \right) \right), \quad (4.13)$$

$$\hat{\mathbf{G}}_{i,j+1/2} = \frac{1}{2} \left(\mathbf{G}_{i,j+1/2}^- + \mathbf{G}_{i,j+1/2}^+ - \alpha_{i,j+\frac{1}{2}} \left(\mathbf{U}_{i,j+1/2}^+ - \mathbf{U}_{i,j+1/2}^- \right) \right), \quad (4.14)$$

where $\alpha_{i+\frac{1}{2},j}$ is defined as (4.17) and $\alpha_{i,j+\frac{1}{2}}$ is defined as (4.18) to ensure the PP property.

For $M_3 = \mathbf{U}_{i,j}^* + \frac{K^2}{r^2} \Delta t^2 \dot{F}(\mathbf{U}_{i,j}^*) = \mathbf{U}_j^* - \frac{K^2}{r^2} \Delta t^2 (H(\mathbf{U}_{i,j}^*)_x + G(\mathbf{U}_{i,j}^*)_y)$, the DG scheme at time level t^n is similar to M_2 .

Theorem 4.2. *For the fourth order $S_2D_2O_4$ DG scheme of the two dimensional Euler equations using the fluxes (4.13) and (4.14), given $\mathbf{U}^n \in G$, under the time step constraint below, the cell average $\bar{\mathbf{U}}^{n+1} \in G$*

$$\frac{\Delta t}{\Delta x} \max_{i,j} \| |u| + c \|_\infty \leq \frac{r}{2} \hat{\omega}_1, \quad \frac{\Delta t^2}{\Delta x^2} \max_{i,j} \left\{ \alpha_{i+\frac{1}{2},j}, \phi_{i+\frac{1}{2},j} \right\} \leq \frac{r^2}{2K^2} \hat{\omega}_1$$

$$\frac{\Delta t}{\Delta y} \max_{i,j} \| |v| + c \|_\infty \leq \frac{r}{2} \widehat{\omega}_1, \quad \frac{\Delta t^2}{\Delta y^2} \max_{i,j} \left\{ \alpha_{i,j+\frac{1}{2}}, \phi_{i,j+\frac{1}{2}} \right\} \leq \frac{r^2}{2K^2} \widehat{\omega}_1$$

Proof. Take the test function $v_h = 1$ on $K_{i,j}$ and zero anywhere else in the scheme (4.11) and (4.12) and denote $\lambda_x = \frac{\Delta t}{\Delta x}$, $\lambda_y = \frac{\Delta t}{\Delta y}$, we obtain the equation satisfied by the cell average of \mathbf{U}^* in the cell $K_{i,j}$

$$\bar{\mathbf{U}}_{i,j}^* = \left(1 - \frac{4rK^2 + r^2}{8K^2} \right) \bar{\mathbf{U}}_{i,j}^n + \frac{r}{2} (\mathbf{R}_1 + \mathbf{R}_3) + \frac{r^2}{8K^2} (\mathbf{R}_2 + \mathbf{R}_4) \quad (4.15)$$

where

$$\begin{aligned} \mathbf{R}_1 &= \frac{1}{2} \bar{\mathbf{U}}_{i,j}^n - \frac{\lambda_x}{r} \frac{1}{\Delta y} \int_{y_{j-\frac{1}{2}}}^{y_{j+\frac{1}{2}}} \widehat{\mathbf{f}}_{i+\frac{1}{2},j}^{\text{LF}} dy + \frac{\lambda_x}{r} \frac{1}{\Delta y} \int_{y_{j-\frac{1}{2}}}^{y_{j+\frac{1}{2}}} \widehat{\mathbf{f}}_{i-\frac{1}{2},j}^{\text{LF}} dy \\ \mathbf{R}_2 &= \frac{1}{2} \bar{\mathbf{U}}_{i,j}^n - \frac{K^2}{r^2} \lambda_x^2 \frac{1}{\Delta y} \int_{y_{j-\frac{1}{2}}}^{y_{j+\frac{1}{2}}} \widehat{\mathbf{H}}_{i+\frac{1}{2},j} dy + \frac{K^2}{r^2} \lambda_x^2 \frac{1}{\Delta y} \int_{y_{j-\frac{1}{2}}}^{y_{j+\frac{1}{2}}} \widehat{\mathbf{H}}_{i-\frac{1}{2},j} dy \\ \mathbf{R}_3 &= \frac{1}{2} \bar{\mathbf{U}}_{i,j}^n - \frac{\lambda_y}{r} \frac{1}{\Delta x} \int_{x_{i-\frac{1}{2}}}^{x_{i+\frac{1}{2}}} \widehat{\mathbf{g}}_{i,j+\frac{1}{2}}^{\text{LF}} dx + \frac{\lambda_y}{r} \frac{1}{\Delta x} \int_{x_{i-\frac{1}{2}}}^{x_{i+\frac{1}{2}}} \widehat{\mathbf{g}}_{i,j-\frac{1}{2}}^{\text{LF}} dx \\ \mathbf{R}_4 &= \frac{1}{2} \bar{\mathbf{U}}_{i,j}^n - \frac{K^2}{r^2} \lambda_y^2 \frac{1}{\Delta x} \int_{x_{i-\frac{1}{2}}}^{x_{i+\frac{1}{2}}} \widehat{\mathbf{G}}_{i,j+\frac{1}{2}} dx + \frac{K^2}{r^2} \lambda_y^2 \frac{1}{\Delta x} \int_{x_{i-\frac{1}{2}}}^{x_{i+\frac{1}{2}}} \widehat{\mathbf{G}}_{i,j-\frac{1}{2}} dx \end{aligned}$$

with

$$\bar{\mathbf{U}}_{ij}^n = \sum_{\eta=1}^{2N_q-1} \sum_{\delta=1}^{2N_q-1} \widehat{w}_\eta \widehat{w}_\delta \mathbf{U}_{\eta,\delta} \quad (4.16)$$

According to [51], we have $\mathbf{R}_1 \in G$ and $\mathbf{R}_3 \in G$, under the condition $\lambda_x \leq \frac{r\widehat{\omega}_1}{2 \max_{i,j} \| |u| + c \|_\infty}$, $\lambda_y \leq \frac{r\widehat{\omega}_1}{2 \max_{i,j} \| |v| + c \|_\infty}$. Next based on the formula (4.16) and the flux (4.13), we can obtain

$$\begin{aligned} \mathbf{R}_2 &= \frac{1}{2} \sum_{\eta=2}^{2N_q-2} \sum_{\delta=1}^{2N_q-1} \widehat{\omega}_\eta \widehat{\omega}_\delta \mathbf{U}_{\eta,\delta} \\ &+ \frac{1}{2} \sum_{\delta=1}^{2N_q-1} \widehat{\omega}_\delta \left[(\widehat{\omega}_{2N_q-1} - \frac{K^2}{r^2} \lambda_x^2 \alpha_{i+\frac{1}{2},\delta}) \mathbf{U}_{i+\frac{1}{2},\delta}^- - \frac{K^2}{r^2} \lambda_x^2 \mathbf{H}_{i+\frac{1}{2},\delta}^- \right] \\ &+ \frac{1}{2} \sum_{\delta=1}^{2N_q-1} \widehat{\omega}_\delta \left[(\widehat{\omega}_1 - \frac{K^2}{r^2} \lambda_x^2 \alpha_{i-\frac{1}{2},\delta}) \mathbf{U}_{i-\frac{1}{2},\delta}^+ + \frac{K^2}{r^2} \lambda_x^2 \mathbf{H}_{i-\frac{1}{2},\delta}^+ \right] \\ &+ \frac{K^2}{2r^2} \lambda_x^2 \sum_{\delta=1}^{2N_q-1} \widehat{\omega}_\delta \left[\alpha_{i+\frac{1}{2},\delta} \mathbf{U}_{i+\frac{1}{2},\delta}^- - \mathbf{H}_{i+\frac{1}{2},\delta}^- \right] \\ &+ \frac{K^2}{2r^2} \lambda_x^2 \sum_{\delta=1}^{2N_q-1} \widehat{\omega}_\delta \left[\alpha_{i-\frac{1}{2},\delta} \mathbf{U}_{i-\frac{1}{2},\delta}^+ + \mathbf{H}_{i-\frac{1}{2},\delta}^+ \right] \end{aligned}$$

where the range of the positive parameter $\alpha_{i+\frac{1}{2},j}$ is determined in the similar way as (4.9):

$$\alpha_{i+\frac{1}{2},j} \geq \max_{\mathbf{U}_{i+\frac{1}{2},j}^-, \mathbf{U}_{i+\frac{1}{2},j}^+} \left[|N_1| + \frac{1}{2\rho^2 e} \left(\sqrt{\rho^2(O_1 - uP_1 - vQ_1)^2 + 2(P_1^2 + Q_1^2)\rho^2 e} + \rho|O_1 - uP_1 - vQ_1| \right) \right], \quad (4.17)$$

with

$$N_1 = \frac{A}{\rho}, \quad O_1 = D - \frac{E}{\rho}A, \quad P_1 = B - Au, \quad Q_1 = C - Av.$$

Here α is taken to be the value that satisfies the equal sign in the inequality (4.17).

Based on the compressible Euler equations in one dimension, when λ_x satisfies $\frac{K^2}{r^2}\lambda_x^2 \max_{i,j} \alpha_{i+\frac{1}{2},j} \leq \frac{1}{2}\widehat{\omega}_1$, we have

$$\begin{aligned} \mathbf{U}_{i-\frac{1}{2},\delta}^-, \mathbf{U}_{i+\frac{1}{2},\delta}^+ \in G &\Rightarrow \mathbf{U}_{i-\frac{1}{2},\delta}^- + \alpha_{i-\frac{1}{2},\delta}^{-1} \mathbf{H} \left(\mathbf{U}_{i-\frac{1}{2},\delta}^- \right) \in G, \quad \mathbf{U}_{i+\frac{1}{2},\delta}^+ - \alpha_{i+\frac{1}{2},\delta}^{-1} \mathbf{H} \left(\mathbf{U}_{i+\frac{1}{2},\delta}^+ \right) \in G, \\ \mathbf{U}_{i-\frac{1}{2},\delta}^+ \in G &\Rightarrow \mathbf{U}_{i-\frac{1}{2},\delta}^+ + \frac{K^2}{r^2} \lambda_x^2 \left(\widehat{\omega}_1 - \frac{K^2}{r^2} \lambda_x^2 \alpha_{i-\frac{1}{2},\delta} \right)^{-1} \mathbf{H} \left(\mathbf{U}_{i-\frac{1}{2},\delta}^+ \right) \in G \\ \mathbf{U}_{i+\frac{1}{2},\delta}^- \in G &\Rightarrow \mathbf{U}_{i+\frac{1}{2},\delta}^- - \frac{K^2}{r^2} \lambda_x^2 \left(\widehat{\omega}_{2N_q-1} - \frac{K^2}{r^2} \lambda_x^2 \alpha_{i+\frac{1}{2},\delta} \right)^{-1} \mathbf{H} \left(\mathbf{U}_{i+\frac{1}{2},\delta}^- \right) \in G. \end{aligned}$$

For the positivity of R_4 , we have similar conclusion, and $\alpha_{i,j+\frac{1}{2}}$ is defined as

$$\alpha_{i,j+\frac{1}{2}} \geq \max_{\mathbf{U}_{i,j+\frac{1}{2}}^-, \mathbf{U}_{i,j+\frac{1}{2}}^+} \left[|N_2| + \frac{1}{2\rho^2 e} \left(\sqrt{\rho^2(O_2 - uP_2 - vQ_2)^2 + 2(P_2^2 + Q_2^2)\rho^2 e} + \rho|O_2 - uP_2 - vQ_2| \right) \right], \quad (4.18)$$

with

$$N_2 = \frac{J}{\rho}, \quad O_2 = M - \frac{E}{\rho}J, \quad P_2 = K - Ju, \quad Q_2 = L - Jv.$$

Then under the PP condition below, we have $\bar{\mathbf{U}}^* \in G$.

$$\begin{aligned} \frac{\Delta t}{\Delta x} \max_{i,j} \| |u| + c \|_\infty &\leq \frac{r}{2} \widehat{\omega}_1, & \frac{\Delta t^2}{\Delta x^2} \max_{i,j} \alpha_{i+\frac{1}{2},j} &\leq \frac{r^2}{2K^2} \widehat{\omega}_1 \\ \frac{\Delta t}{\Delta y} \max_{i,j} \| |v| + c \|_\infty &\leq \frac{r}{2} \widehat{\omega}_1, & \frac{\Delta t^2}{\Delta y^2} \max_{i,j} \alpha_{i,j+\frac{1}{2}} &\leq \frac{r^2}{2K^2} \widehat{\omega}_1 \end{aligned}$$

The cell average of \mathbf{U}^{n+1} on cell I_j can be expressed as

$$\bar{\mathbf{U}}_j^{n+1} = r \left(1 - \frac{r^2}{6K^2} \right) (\mathbf{R}_1 + \mathbf{R}_3) + \frac{r^2 (4K^2 - r^2)}{24K^4} (\mathbf{R}_2 + \mathbf{R}_4) + \frac{r^2}{3K^2} (\mathbf{R}_5 + \mathbf{R}_6)$$

where

$$\mathbf{R}_5 = \frac{1}{2} \bar{\mathbf{U}}_{i,j}^* - \frac{K^2}{r^2} \lambda_x^2 \frac{1}{\Delta y} \int_{y_{j-\frac{1}{2}}}^{y_{j+\frac{1}{2}}} \widehat{\mathbf{H}}_{i+\frac{1}{2},j}^* dy + \frac{K^2}{r^2} \lambda_x^2 \frac{1}{\Delta y} \int_{y_{j-\frac{1}{2}}}^{y_{j+\frac{1}{2}}} \widehat{\mathbf{H}}_{i-\frac{1}{2},j}^* dy$$

$$R_6 = \frac{1}{2} \bar{U}_{i,j}^* - \frac{K^2}{r^2} \lambda_y^2 \frac{1}{\Delta x} \int_{x_{i-\frac{1}{2}}}^{x_{i+\frac{1}{2}}} \widehat{\mathbf{M}}_{i,j+\frac{1}{2}}^* dx + \frac{K^2}{r^2} \lambda_y^2 \frac{1}{\Delta x} \int_{x_{i-\frac{1}{2}}}^{x_{i+\frac{1}{2}}} \widehat{\mathbf{M}}_{i,j-\frac{1}{2}}^* dx$$

Similarly, the time step satisfies the following time step constraint:

$$\frac{K^2}{r^2} \lambda_x^2 \max_{i,j} \phi_{i+\frac{1}{2},j} \leq \frac{1}{2} \widehat{\omega}_1, \quad \frac{K^2}{r^2} \lambda_y^2 \max_{i,j} \phi_{i,j+\frac{1}{2}} \leq \frac{1}{2} \widehat{\omega}_1$$

Therefore, the complete PP time step condition is:

$$\begin{aligned} \frac{\Delta t}{\Delta x} \max_{i,j} \| |u| + c \|_\infty &\leq \frac{r}{2} \widehat{\omega}_1, & \frac{\Delta t^2}{\Delta x^2} \max_{i,j} \left\{ \alpha_{i+\frac{1}{2},j}, \phi_{i+\frac{1}{2},j} \right\} &\leq \frac{r^2}{2K^2} \widehat{\omega}_1 \\ \frac{\Delta t}{\Delta y} \max_{i,j} \| |v| + c \|_\infty &\leq \frac{r}{2} \widehat{\omega}_1, & \frac{\Delta t^2}{\Delta y^2} \max_{i,j} \left\{ \alpha_{i,j+\frac{1}{2}}, \phi_{i,j+\frac{1}{2}} \right\} &\leq \frac{r^2}{2K^2} \widehat{\omega}_1 \end{aligned}$$

5 The positivity-preserving limiter

In the Sections 3 and 4, we have constructed the PP $S_2D_2O_4$ DG schemes for hyperbolic equations of scalar and system cases. We conclude that provided these conditions in the above theorems are satisfied by the entire solution at the previous time level, the cell averages of the target variables are positive under appropriate time-step conditions. Then to close the cycle of our algorithm, we use the PP limiter to achieve the positivity for the entire solution.

The PP limiter for scalar conservation laws is as follows. Given $u \in V$ with $\bar{u}_j \geq 0$, $j = 1, 2, \dots, N$, define the modified solution $\tilde{u} \in V$:

$$\tilde{u}_j(x) = \theta_j (u_j(x) - \bar{u}_j) + \bar{u}_j, \quad \theta_j = \min \left\{ 1, \frac{\bar{u}_j - \epsilon_1}{\bar{u}_j - m_j} \right\}$$

$$m_j = \min_{1 \leq \mu \leq 2N_q-1} u_j(\hat{x}_j^\mu), \quad j = 1, 2, \dots, N$$

where ϵ_1 is defined in the Remark 1. Then the modified solution $\tilde{u}_j(x) \geq 0$, $j = 1, \dots, N$ and it preserves the cell average unchanged. Moreover, it was proved in [49] that such a limiter does not destroy the original high order accuracy.

For the solution $\mathbf{U} = (\rho, m, E)^T \in V \times V \times V$ of the Euler equations with $\bar{\mathbf{U}}_j \in G$, $j = 1, 2, \dots, N$, we adopt the following modified limiting process in [43].

First, enforce the positivity of the density function ρ by,

$$\hat{\rho}_j(x) = \theta_j^\rho (\rho_j(x) - \bar{\rho}_j) + \bar{\rho}_j, \quad \theta_j^\rho = \min \left\{ 1, \frac{\bar{\rho}_j}{\bar{\rho}_j - \min_{1 \leq \mu \leq 2N_q-1} \rho(\hat{x}_j^\mu)} \right\}, \quad j = 1, 2, \dots, N$$

Then let $\hat{\mathbf{U}}_j = (\hat{\rho}_j, m_j, E_j)^T$ and define

$$\tilde{\mathbf{U}}_j(x) = \theta_j^e \left(\hat{\mathbf{U}}_j(x) - \bar{\mathbf{U}}_j \right) + \bar{\mathbf{U}}_j, \theta_j^e = \min \left\{ 1, \frac{\rho e(\bar{\mathbf{U}}_j)}{\rho e(\bar{\mathbf{U}}_j) - \min_{1 \leq \mu \leq 2N_q-1} \rho e(\hat{\mathbf{U}}_j(\hat{x}_j^\mu))} \right\}, j = 1, 2, \dots, N$$

Because of the concaveness of the function $\rho e(\mathbf{U})$, we obtain $\tilde{\mathbf{U}}_j(\hat{x}_j^\mu) \in G, \mu = 1, 2, \dots, 2N_q - 1$, and also it does not destroy accuracy of the solution, see the detailed proof in [51] and [43].

The PP limiter has the same form in multi-dimensions. To enhance the stability of algorithms, we can set a threshold $\epsilon_2 = 10^{-10}$ and let $\tilde{u}_j = \bar{u}_j$ if $\bar{u}_j < \epsilon_2$ for scalar conservation law, and $\tilde{\mathbf{U}}_j = \bar{\mathbf{U}}_j$ if $\bar{\rho}_j < \epsilon_2$ or $\rho e(\bar{\mathbf{U}}_j) < \epsilon_2$ for the Euler equations.

6 Numerical tests

We test the PP $S_2D_2O_4$ DG schemes for the scalar conservation laws for one-dimension and two-dimension cases, as well as for the compressible Euler equations of gas dynamics, respectively. We verify the accuracy and effectiveness of the PP $S_2D_2O_4$ DG schemes through several tests.

Note that when ρ is near zero, the computation of $u_x, u_y, v_x, v_y, u_t, v_t, u, v$ is problematic. To ensure the stability of the algorithm, here we make $u_x, u_y, v_x, v_y, u_t, v_t, u, v$ all equal to 0 when $\rho < \epsilon_2$.

All the tests use only the PP limiter for preserving positivity, except for Example 6.13. For Example 6.13, the numerical solution is highly oscillatory if only the PP limiter is used, thus the TVB limiter is also used to reduce oscillations in this test.

6.1 Scalar conservation laws

Example 6.1 (The accuracy and positivity test for the 1D linear equation). We solve the linear equation $u_t + u_x = 0$ in the domain $\Omega = [0, 1]$ with periodic boundary conditions.

First, we take the smooth initial condition $u_0(x) = \sin^{16}(\pi x)$ and the terminal time

$T = 1$. The errors and order of convergence of the problem with the smooth initial condition are given in Table 6.1. In this table, N_c is the percentage of the cells using the PP limiter, N_h is the percentage of halving the time step, and N_m is the percentage of using the PP flux. These notations remain the same for the following examples as well. We can observe the PP flux does not affect the fourth order of accuracy and there is a certain amount of halving of the time steps.

Table 6.1: Results of Example 6.1 with the smooth initial condition at $T = 1$.

Mesh	L^1	order	L^2	order	L^∞	order	$N_c(\%)$	$N_h(\%)$	$N_m(\%)$
20	3.6631E-03	–	5.2036E-03	–	2.1757E-02	–	24.9482	5.6995	5.6995
40	5.0893E-05	6.1695	8.8852E-05	5.8719	4.3806E-04	5.6342	8.1201	3.9578	3.9578
80	2.9388E-06	4.1141	5.1228E-06	4.1164	2.5676E-05	4.0926	6.6845	0.9524	1.0884
160	1.8350E-07	4.0014	3.1718E-07	4.0136	1.6013E-06	4.0032	0.3677	0	0
320	1.1451E-08	4.0023	1.9796E-08	4.0020	9.9135E-08	4.0137	0.0001	0	0
640	7.1616E-10	3.9990	1.2370E-09	4.0003	6.2004E-09	3.9990	0	0	0

Then to test the effect of the positivity-preserving property, we adopt the discontinuous initial condition

$$u_0(x) = \begin{cases} 1, & 0 \leq x < \frac{1}{4} \\ 0, & \frac{1}{4} \leq x < \frac{3}{4} \\ 1, & \frac{3}{4} \leq x \leq 1 \end{cases}$$

and take the terminal time $T = 1$. The result of the problem with the discontinuous initial condition is shown in Fig. 2. We can observe that the result with the PP limiter can eliminate the negative values compared with the result without the PP limiter.

Example 6.2 (The accuracy and positivity test for the 1D Burgers equation).

We solve the Burgers equation $u_t + \left(\frac{u^2}{2}\right)_x = 0$ in the domain $\Omega = [0, 1.4]$ with the initial condition

$$u_0(x) = \begin{cases} 0, & 0 \leq x < 0.4 \\ \sin^6(\pi(x - 0.4)), & 0.4 \leq x \leq 1.4 \end{cases}$$

and periodic boundary conditions. We list the errors and order of convergence at $T = 0.1$ in Table 6.2, which shows fourth order accuracy. This confirms that the PP flux does not affect the high order accuracy. No rewinding of computation happens for this test.

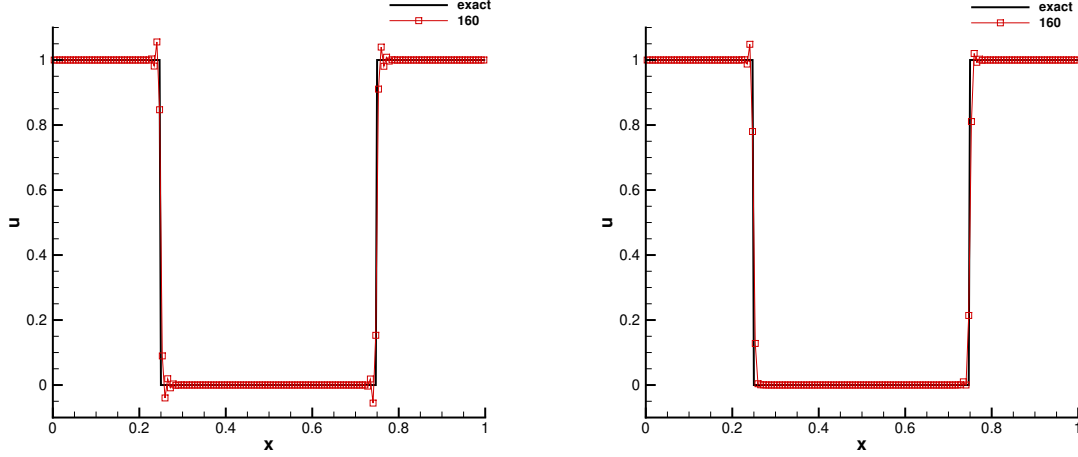


Figure 2: Results of Example 6.1 for the discontinuous initial condition at $T = 1$ on the 160 grid. Left: without the PP limiter; Right: with the PP limiter.

Table 6.2: Results of Example 6.2 for the smooth initial solution at $T = 0.1$.

Mesh	L^1	order	L^2	order	L^∞	order	$N_c(\%)$	$N_h(\%)$	$N_m(\%)$
20	5.7510E-05	–	1.9223E-04	–	2.3147E-03	–	23.1731	0	100
40	1.0010E-05	2.5224	3.9430E-05	2.2855	4.0515E-04	2.5143	11.0577	0	25.0000
80	4.8155E-07	4.3775	2.0319E-06	4.2784	3.0082E-05	3.7515	2.6202	0	3.8462
160	2.9548E-08	4.0266	1.2233E-07	4.0539	1.6979E-06	4.1471	1.2680	0	0.4808
320	1.8346E-09	4.0096	7.5689E-09	4.0146	1.1134E-07	3.9306	0.4695	0	0
640	1.1400E-10	4.0083	4.7215E-10	4.0028	7.0245E-09	3.9865	0.0000	0	0

Next, we adopt the discontinuous initial condition

$$u_0(x) = \begin{cases} 1, & 0 \leq x < \frac{1}{4} \\ 0, & \frac{1}{4} \leq x < \frac{3}{4} \\ 1, & \frac{3}{4} \leq x \leq 1 \end{cases}$$

in the domain $\Omega = [0, 1.4]$ and take the terminal time $T = 0.1$ and $N = 160$. The results of the problem with the discontinuous initial condition are shown in Fig. 3. The effect of the PP property is obvious by comparing the locally enlarged images.

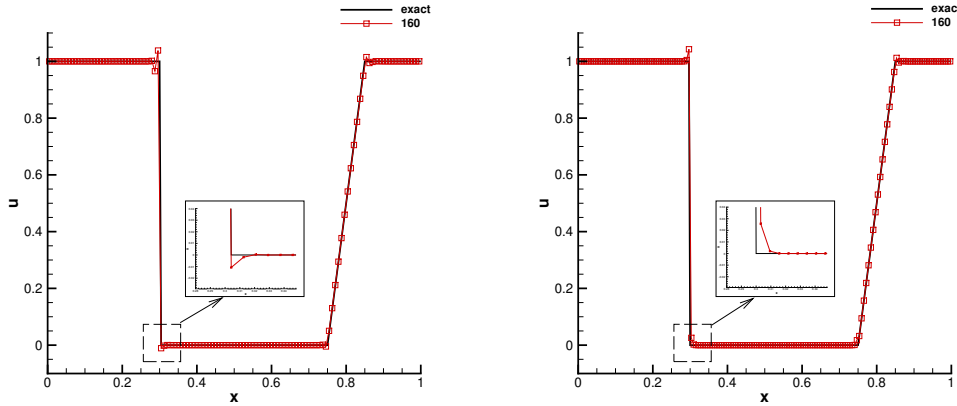


Figure 3: Results of Example 6.2 for the discontinuous initial condition at $T = 0.1$ on the 160 grid. Left: without the PP limiter; Right: with the PP limiter.

Example 6.3 (The accuracy and positivity test for the 2D linear equation).

We solve the two dimensional linear equation $u_t + u_x + u_y = 0$ in the domain $\Omega = [0, 2] \times [0, 2]$ with periodic boundary conditions.

We first take the smooth initial condition $u_0(x, y) = \sin^{12}(\pi(x+y))$ and the terminal time $T = 0.1$ to test the accuracy of the $S_2D_2O_4$ DG scheme. The errors and order of convergence for the smooth initial condition are given in Table 6.3, from which the fourth order accuracy can be observed. The case of halving time steps does not happen in this test.

Next, we change the initial condition into the discontinuous initial condition

$$u_0(x) = \begin{cases} 0, & \frac{1}{4} \leq \frac{(x+y)}{2} < \frac{3}{4} \\ 1, & \text{otherwise} \end{cases} \quad \text{and} \quad \frac{5}{4} \leq \frac{(x+y)}{2} < \frac{7}{4}$$

and take the terminal time $T = 0.1$. The results of the problem are shown in Fig. 4, where we take $N = 160$ for an $N \times N$ mesh and plot the numerical solution at the Gauss integration

Table 6.3: Results of Example 6.3 for the smooth initial solution at $T = 0.1$.

Mesh	L^1	order	L^2	order	L^∞	order	$N_c(\%)$	$N_h(\%)$	$N_m(\%)$
20	9.3777E-03	3.4909	1.3062E-02	3.4820	5.2502E-02	2.8967	48.4211	0	5.2632
40	6.5014E-04	3.8504	1.1777E-03	3.4714	6.2921E-03	3.0607	33.2432	0	8.1081
80	1.2006E-05	5.7589	2.8990E-05	5.3442	3.3913E-04	4.2136	18.2534	0	5.4795
160	6.7880E-07	4.1446	1.8062E-06	4.0045	2.1323E-05	3.9914	8.5188	0	2.0548
320	4.1539E-08	4.0305	1.1333E-07	3.9944	1.3368E-06	3.9955	0.2889	0	0
640	2.6113E-09	3.9916	7.0651E-09	4.0037	8.3344E-08	4.0036	0	0	0

points cut along the diagonal ($x = y$) and r is the distance from the origin. We can see the PP limiter works effectively by comparison.

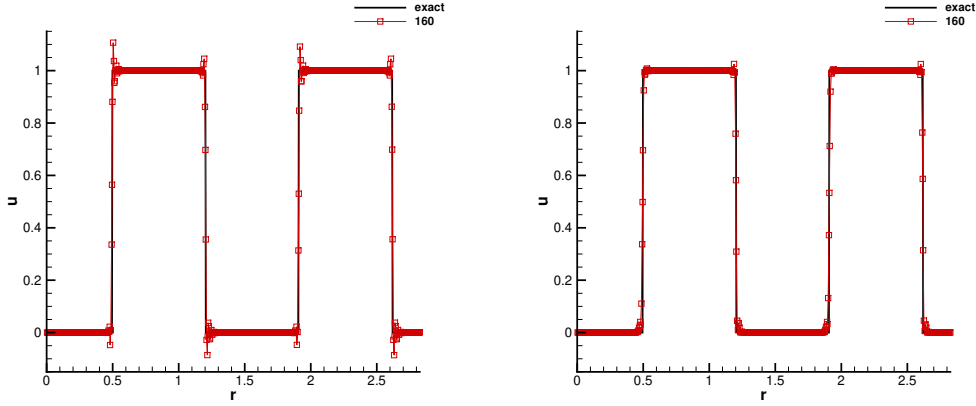


Figure 4: Results of Example 6.3 for the discontinuous initial condition at $T = 0.1$ on the 160 grid. Left: without the PP limiter; Right: with the PP limiter.

Example 6.4 (The accuracy and positivity test for the 2D Burgers equation).

We solve the two dimensional Burgers equation $u_t + \left(\frac{u^2}{2}\right)_x + \left(\frac{u^2}{2}\right)_y = 0$ in the domain $\Omega = [0, 2] \times [0, 2]$ with the initial condition $u_0(x, y) = \sin^{16}(\pi(x + y))$ and periodic boundary conditions.

We list the errors and order of convergence at $T = 0.01$ under the L^1 , L^2 and L^∞ norms in Table 6.4. The fourth order accuracy is observed which suggests the PP flux does not influence the order of accuracy. The time step is not be halved in this test case.

Table 6.4: Results of Example 6.4 with the smooth initial solution at $T = 0.01$.

Mesh	L^1	order	L^2	order	L^∞	order	$N_c(\%)$	$N_h(\%)$	$N_m(\%)$
20	8.2607E-03	–	1.5109E-01	–	1.8472E-02	–	70.0000	0	50.0000
40	6.2254E-04	3.7300	1.2182E-02	3.6325	1.3803E-03	3.7423	27.5000	0	75.0000
80	2.0461E-05	4.9272	9.9779E-04	3.6099	5.7613E-05	4.5824	8.1250	0	75.0000
160	1.2127E-06	4.0766	6.5223E-05	3.9353	3.6636E-06	3.9751	3.5833	0	26.6667
320	7.7396E-08	3.9698	4.7467E-06	3.7804	2.4416E-07	3.9073	2.1250	0	0
640	4.8177E-09	4.0058	3.0484E-07	3.9608	1.5423E-08	3.9847	0	0	0

To test the effect of preserving positivity, we adopt a discontinuous initial condition

$$u_0(x) = \begin{cases} 0, & \frac{1}{4} \leq \frac{(x+y)}{2} < \frac{3}{4} \quad \text{and} \quad \frac{5}{4} \leq \frac{(x+y)}{2} < \frac{7}{4} \\ 1, & \text{otherwise} \end{cases}$$

and take the terminal time $T = 0.1$ and $N = 160$. The results of the problem are shown in Fig. 5, where the comparison with the exact solution and the result of the unlimited numerical solution are given along the diagonal ($x = y$). We can see the PP limiter works effectively.

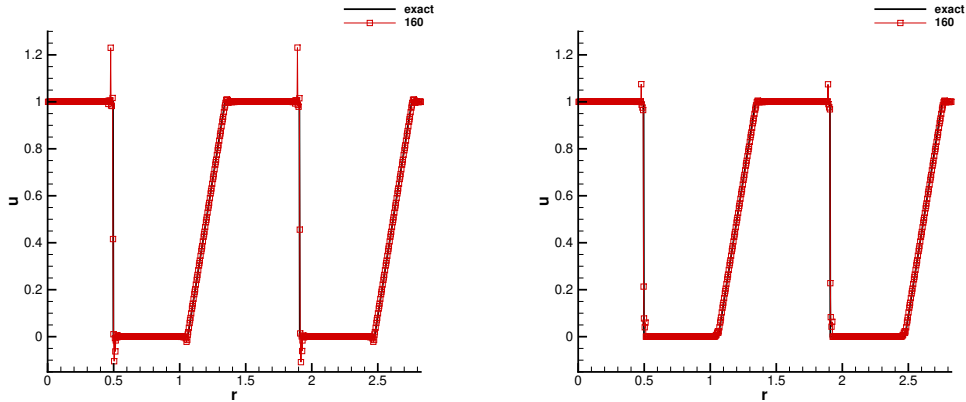


Figure 5: Results of Example 6.4 for the discontinuous initial condition at $T = 0.1$ on the 160 grid. Left: without the PP limiter; Right: with the PP limiter.

6.2 The Euler equations

Example 6.5 (An accuracy test for the 1D Euler equation). We solve the one dimensional problem in the domain $[0, 3]$ with the initial condition:

$$\rho(x, 0) = \frac{\mu(x, 0)}{\sqrt{12}}, \quad u(x, 0) = \sqrt{\gamma}\rho(x, y, 0), \quad p(x, 0) = \rho(x, 0)^\gamma$$

and periodic boundary conditions. The ratio of specific heat is $\gamma = 3$.

The exact solution of the problem is

$$\rho(x, t) = \frac{\mu(x, t)}{\sqrt{12}}, \quad u(x, t) = \sqrt{\gamma}\rho(x, t), \quad p(x, t) = \rho(x, t)^\gamma$$

where $\mu(x, t)$ is the exact solution of the Burgers equation:

$$\partial_t \mu + \frac{1}{2} \partial_x (\mu^2) = 0, \quad \mu(x, 0) = \begin{cases} 10^{-14}, & 0 < x < 2, \\ \sin(\pi(x - 2))^6 + 10^{-14}, & \text{otherwise} \end{cases}$$

The positivity of density and pressure is preserved with the PP limiter and the fourth order convergence of density at time $T = 0.1$ is shown in Table 6.5. There are some occasions of halving time step.

Table 6.5: Results of Example 6.5 at $T = 0.1$.

Mesh	L^1	order	L^2	order	L^∞	order	$N_c(\%)$	$N_h(\%)$	$N_m(\%)$
10	1.029E-02	–	1.931E-02	–	6.472E-02	–	81.562	25.000	50.000
20	2.155E-03	2.255	6.735E-03	1.520	5.136E-02	0.333	50.357	7.143	28.571
40	3.878E-04	2.475	1.192E-03	2.499	8.777E-03	2.549	30.700	0.000	8.000
80	1.315E-05	4.883	4.156E-05	4.842	3.203E-04	4.776	8.999	0.000	2.041
160	4.345E-07	4.919	1.617E-06	4.684	2.128E-05	3.912	2.353	0.000	0.000
320	1.555E-08	4.805	6.258E-08	4.691	1.240E-06	4.102	0.713	0.000	0.000
640	7.477E-10	4.378	3.209E-09	4.286	6.173E-08	4.328	0.195	0.000	0.000
1280	4.190E-11	4.158	1.900E-10	4.078	3.319E-09	4.217	0.081	0.000	0.000

Example 6.6 (The blast waves problem). We solve the one dimensional problem of the blast waves in the domain $\Omega = [0, 1]$ with the initial condition

$$(\rho_0, u_0, p_0) = \begin{cases} (1, 0, 10^3) & 0 \leq x < 0.1 \\ (1, 0, 10^{-2}) & 0.1 \leq x < 0.9 \\ (1, 0, 10^2), & 0.9 \leq x < 1 \end{cases}$$

and reflective boundary condition. The ratio of specific heat is $\gamma = 1.4$. We plot the density of the cell averages of the numerical solutions at $T = 0.038$ for $N = 200$ and $N = 400$ respectively. The reference solution is computed by the WENO-5 scheme with 16,000 cells. The results are shown in Fig. 6. Since only the PP limiter is used, we can observe some oscillations in the figures.

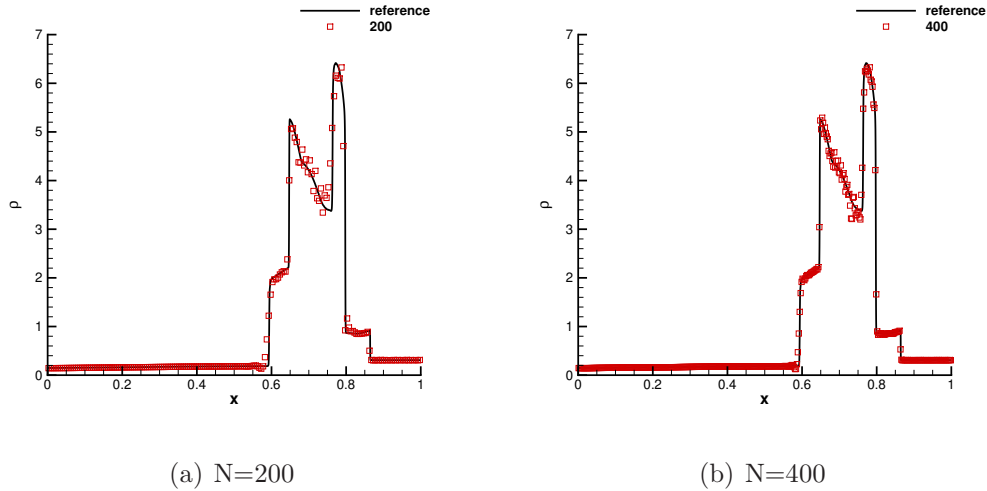
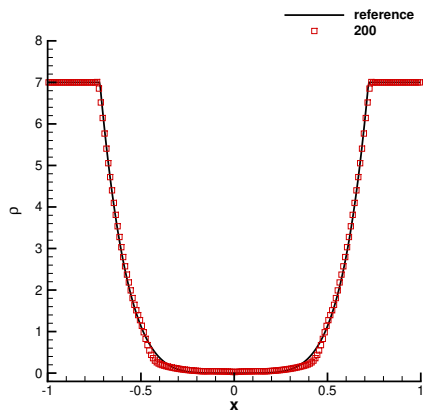


Figure 6: Results of Example 6.6, plot of density at $T=0.038$.

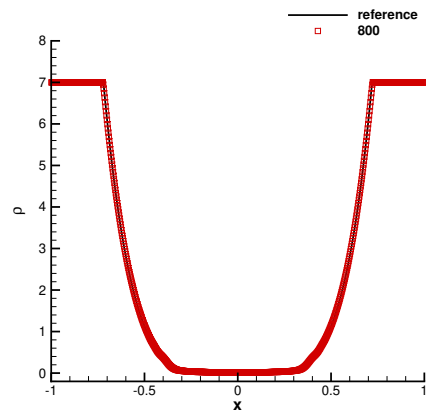
Example 6.7 (The double rarefaction Riemann problem). We solve a double rarefaction Riemann problem in the domain $\Omega = [-1, 1]$ with initial condition

$$(\rho_0, u_0, p_0) = \begin{cases} (7, -1, 0.2), & x < 0 \\ (7, 1, 0.2), & x > 0 \end{cases}$$

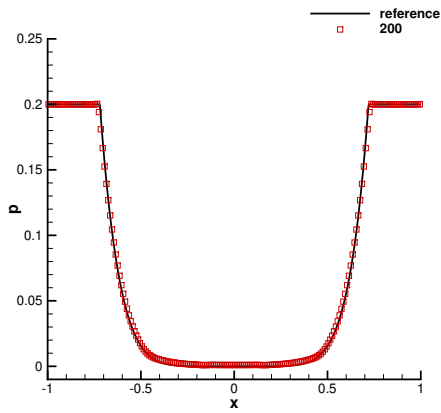
and $\gamma = 1.4$. In this test example, the exact solution will generate vacuum (zero density). The simulation will blow up without the PP limiter in the tests. We plot the density, pressure and velocity of the cell averages of the numerical solution with the PP limiter of this problem at $T = 0.6$ for $N = 200$ and $N = 800$ respectively in Fig. 7. The reference solution is obtained from the exact Riemann solver [40]. We can see that the low pressure and the low density are captured very well and the positivity of density and pressure is preserved.



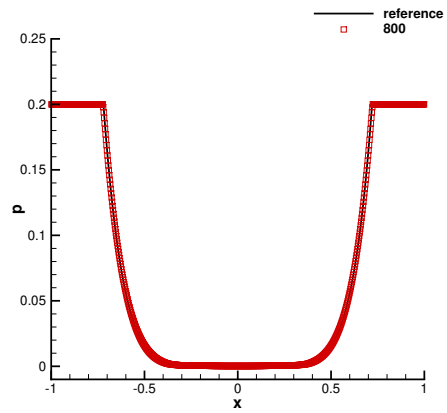
(a) Density



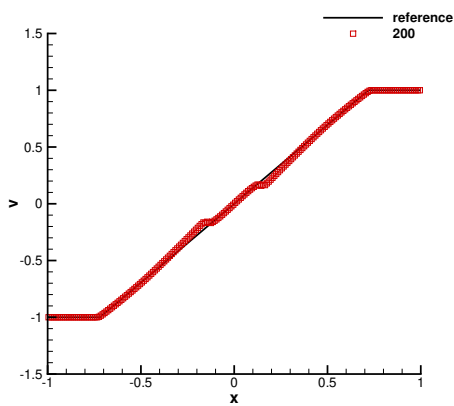
(b) Density



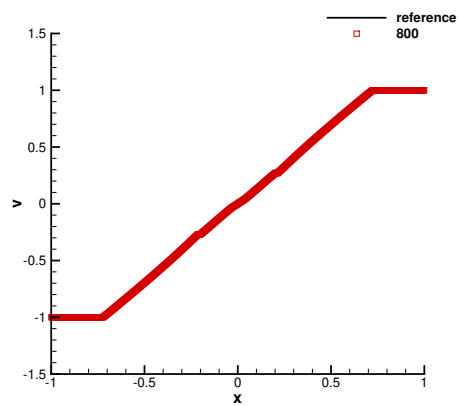
(c) Pressure



(d) Pressure



(e) Velocity



(f) Velocity

Figure 7: Results of Example 6.7, at $T = 0.6$.

Example 6.8 (The Leblanc shock tube Riemann problem). We consider another extreme Riemann problem called the Leblanc shock tube Riemann problem with the initial condition

$$(\rho_0, u_0, p_0) = \begin{cases} (2, 0, 10^9), & x < 0 \\ (10^{-3}, 0, 1), & x > 0 \end{cases}$$

in the domain $\Omega = [-10, 10]$, $\gamma = 1.4$. The simulation will blow up without the PP limiter in the tests.

The numerical results at $T = 0.0001$ for $N = 800$ and $N = 1,600$ are shown respectively in Fig. 8, where the y -axis uses log scales. We obtain the reference solution from the exact Riemann solver [40]. From the figures, we can see that the positivity of density and pressure is preserved.

Example 6.9 (An accuracy test for the 2D Euler equation). We solve the two dimensional problem in the domain $[0, 6] \times [0, 6]$ with the initial condition:

$$\begin{aligned} \rho(x, y, 0) &= \frac{\mu(x, y, 0)}{\sqrt{6}} \\ u(x, y, 0) &= v(x, y, 0) = \sqrt{\frac{\gamma}{2}} \rho(x, y, 0) \\ p(x, y, 0) &= \rho(x, y, 0)^\gamma \end{aligned}$$

with periodic boundary conditions and $\gamma = 3$.

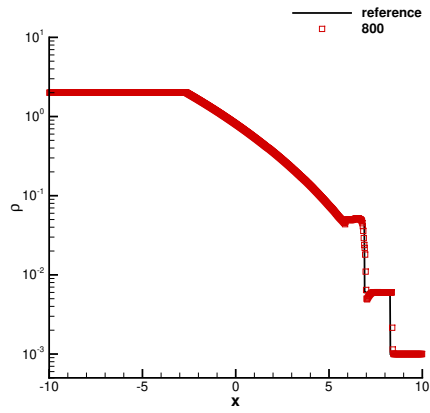
The exact solution of the problem is

$$\rho(x, y, t) = \frac{\mu(x, y, t)}{\sqrt{6}}, \quad u(x, y, t) = v(x, y, t) = \sqrt{\frac{\gamma}{2}} \rho(x, y, t), \quad p(x, y, t) = \rho(x, y, t)^\gamma$$

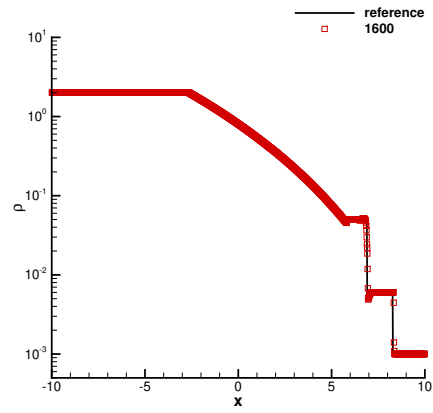
where $\mu(x, y, t)$ is the exact solution of the Burgers equation

$$\partial_t \mu + \frac{1}{2} \partial_x (\mu^2) + \frac{1}{2} \partial_y (\mu^2) = 0, \quad \mu(x, y, 0) = \begin{cases} 10^{-14}, & 0 < \frac{(x+y)}{2} < 2 \quad \text{and} \quad 4 < \frac{(x+y)}{2} < 5, \\ \sin(\pi(\frac{(x+y)}{2} - 2))^6 + 10^{-14}, & \text{otherwise} \end{cases}$$

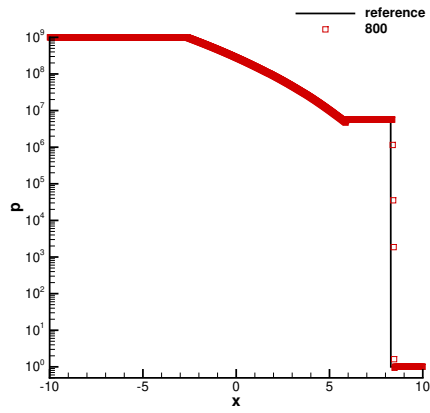
The positivity of density and pressure is preserved during the simulation and the fourth order convergence of density at time $T = 0.01$ is shown in Table 6.6. There are some halved time steps.



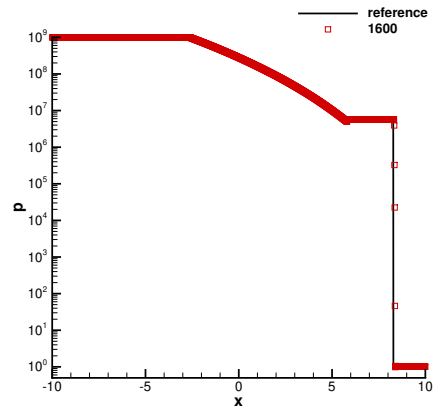
(a) Density, log scale



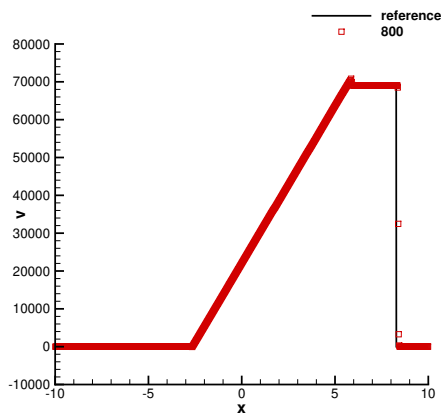
(b) Density, log scale



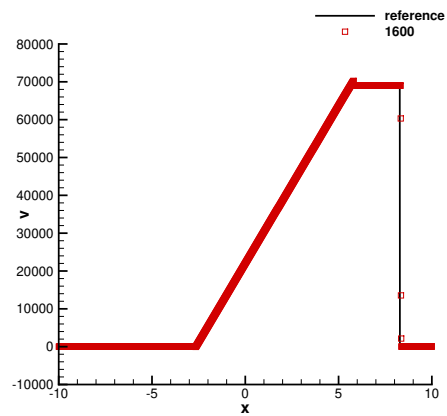
(c) Pressure, log scale



(d) Pressure, log scale



(e) Velocity



(f) Velocity

Figure 8: Results of Example 6.8, at $T = 0.0001$.

Table 6.6: Results of Example 6.8 at $T = 0.01$.

Mesh	L^1	order	L^2	order	L^∞	order	$N_c(\%)$	$N_h(\%)$	$N_m(\%)$
10	7.862E-03	–	2.002E-02	–	1.030E-01	–	88.750	75.000	75.000
20	1.583E-03	2.312	4.749E-03	2.076	6.059E-02	0.766	80.312	50.000	50.000
40	1.549E-04	3.353	6.900E-04	2.783	1.586E-02	1.934	63.594	25.000	25.000
80	8.435E-06	4.199	3.356E-05	4.362	6.535E-04	4.601	53.795	14.286	14.286
160	2.149E-07	5.295	8.076E-07	5.377	3.535E-05	4.209	43.633	0.000	0.000
320	1.261E-08	4.091	4.996E-08	4.015	2.316E-06	3.932	38.379	0.000	0.000

Example 6.10 (The Sedov blast wave problem). The Sedov point-blast wave is a good test for a PP scheme because of the existence of low density and low pressure. We solve the two dimensional Sedov point-blast wave problem [34] in the domain $\Omega = [0, 1.1] \times [0, 1.1]$ with the initial condition

$$\rho_0 = 1, \quad u_0 = v_0 = 0, \quad E_0 = \begin{cases} \frac{0.244816}{\Delta x \Delta y}, & (x, y) \in [0, \Delta x] \times [0, \Delta y] \\ 10^{-12}, & \text{otherwise} \end{cases}$$

and the left and bottom boundary are set as the reflective boundary, and other boundaries are set as the outflow boundary. The ratio of specific heat is $\gamma = 1.4$.

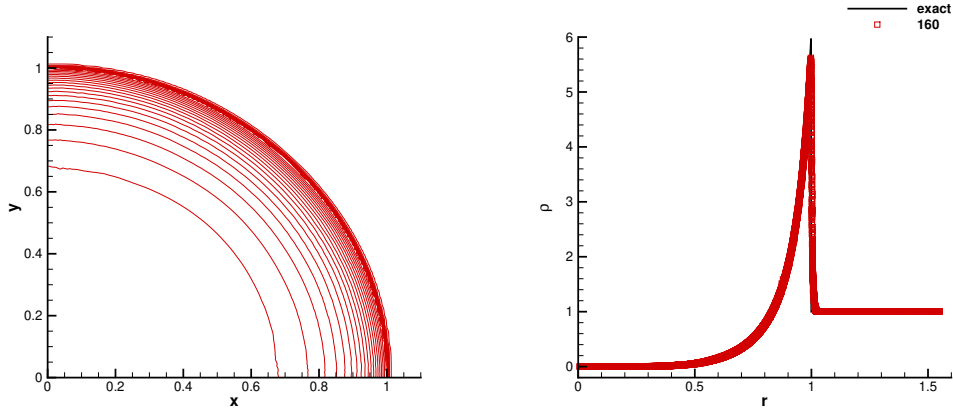
We plot the density on Ω and its projection to the radial coordinate Ω at $T = 1$ on the 160×160 grid, see Fig. 9. The simulation blows up if the PP limiter is not used in this test and we can observe that the positivity of density is preserved and the numerical solution maintains nice radial symmetry.

Example 6.11 (The double Mach reflection problem of a Mach 10 shock)

Consider the two-dimensional double Mach reflection problem with a Mach 10 shock in the domain $\Omega = [0, 4] \times [0, 1]$, with the initial condition

$$(\rho_0, u_0, v_0, p_0) = \begin{cases} \left(8, \frac{33\sqrt{3}}{8}, -\frac{33}{8}, 116.5\right), & y > \sqrt{3}\left(x - \frac{1}{6}\right) \quad (\text{post-shock}) \\ (1.4, 0, 0, 1), & y < \sqrt{3}\left(x - \frac{1}{6}\right) \quad (\text{pre-shock}) \end{cases}$$

The left boundary is set as the inflow boundary, the right boundary is set as the outflow boundary, $\{0 \leq x < \frac{1}{6}, y = 0\}$ on the bottom is the boundary with post-shock condition, $\{\frac{1}{6} < x \leq 4, y = 0\}$ on the bottom is the reflective boundary, and the condition on the top



(a) 20 equally spaced contour lines from 0 to 1. (b) Projection to the radial coordinate.

Figure 9: Results of Example 6.9, plot of density at $T = 1$ on the 160×160 grid.

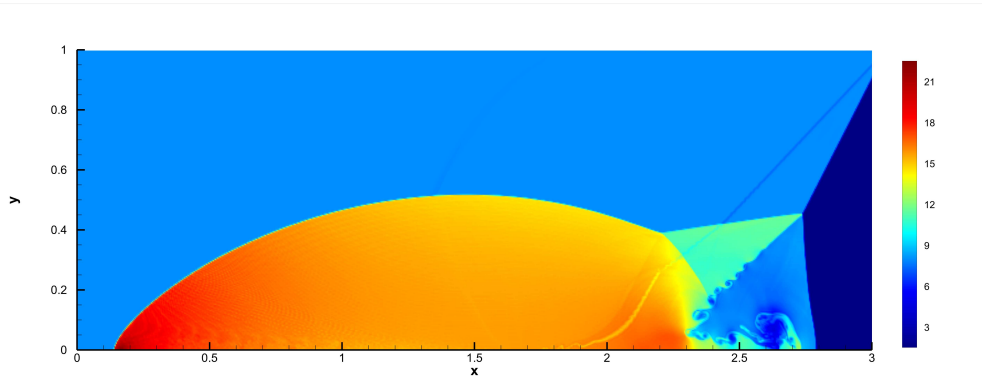
boundary is consistent with the motion of the shock. The results at $T = 0.2$ on the 960×240 grid are shown in Fig. 10 and comparable with the results in [49]. Our $S_2D_2O_4$ DG schemes with only the PP limiter can capture detailed structure by comparison.

Example 6.12 (The shock diffraction problem). We solve the two dimensional problem of shock passing a backward facing corner in the domain $\Omega = [1, 13] \times [0, 11] \cup [0, 1] \times [6, 11]$, with the initial condition

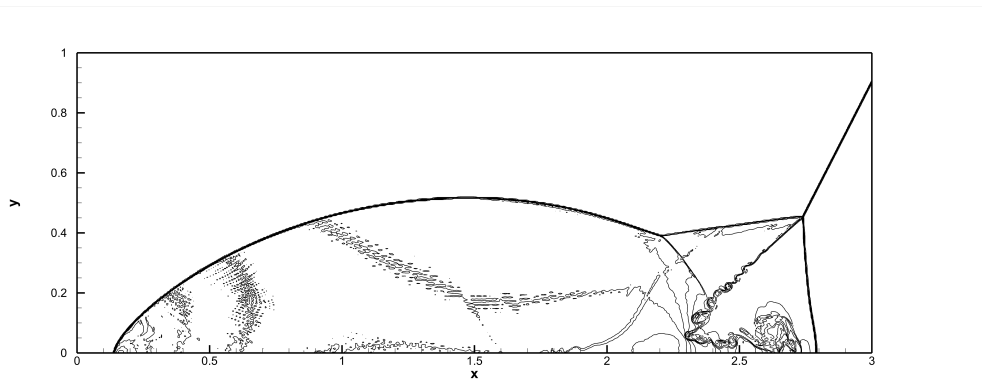
$$(\rho_0, u_0, v_0, p_0) = \begin{cases} (\rho_*, u_*, v_*, p_*), & x < 0.5 \quad (\text{post-shock}) \\ (1.4, 0, 0, 1), & x > 0.5 \quad (\text{pre-shock}) \end{cases}$$

where $(\rho_*, u_*, v_*, p_*) = (7.041132906907898, 4.07794695481336, 0, 30.05945)$. The shock is rightmoving with Mach number 5.09. The boundary $\{x = 0, 6 \leq y \leq 11\}$ is the inflow boundary, $\{0 \leq x \leq 1, y = 6\}$ and $\{x = 1, 0 \leq y \leq 6\}$ are reflection boundaries, $\{x = 13, 0 \leq y \leq 11\}$ and $\{1 \leq x \leq 13, y = 0\}$ are outflow boundaries, and the boundary condition on $\{0 \leq x \leq 13, y = 11\}$ follows the shockwave movement.

The density and pressure at $T = 2.3$ with $\Delta x = \Delta y = \frac{1}{32}$ are presented in Fig. 11. This example is easy to get negative density and pressure below and to the right of the corner without the PP limiter. The results are comparable with those in [49], achieving the positivity of density and pressure.

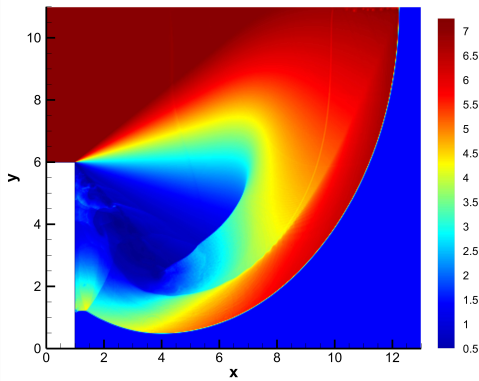


(a) Density on $[0,3] \times [0,1]$

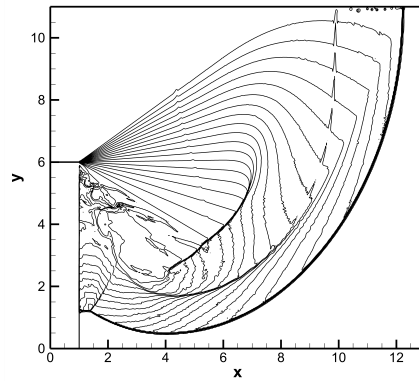


(b) 23 equally spaced contour lines from 1 to 24 for density

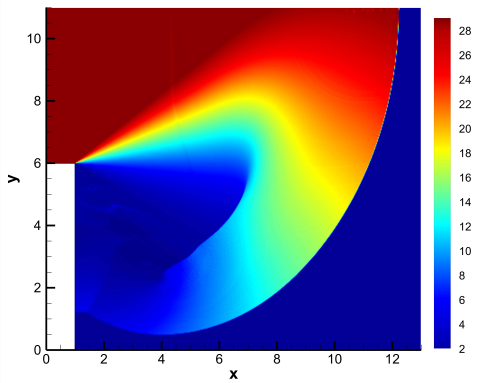
Figure 10: Results of Example 6.10 at $T = 0.2$ on the 960×240 grid.



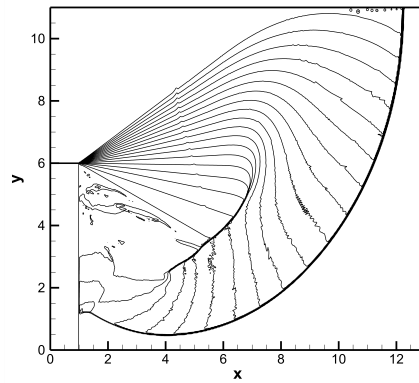
(a) Density in Ω



(b) 20 equally spaced contour lines from 0.474419 to 6.64186 for density



(c) Pressure in Ω



(d) 20 equally spaced contour lines from 0 to 28.401 for pressure

Figure 11: Results of Example 6.12 at $T = 2.3$ with $\Delta x = \Delta y = \frac{1}{32}$.

Example 6.13 (The high Mach number astrophysical jets problem). Consider the two-dimensional astrophysical jets problems with very high Mach number. We set the domain $\Omega = [0, 0.5] \times [0, 0.25]$ with initial condition $\rho_0(x, y) = 0.5$, $u_0(x, y) = v_0(x, y) = 0$, $p_0(x, y) = 0.4127$. The boundary conditions of the right and top are outflow, the bottom boundary is reflective and the left boundary is inflow with $(\rho, u, v, p) = (5, 800, 0, 0.4127)$ if $0 \leq y \leq 0.05$, which corresponds to a jet flow of Mach number 2000, while $(\rho, u, v, p) = (0.5, 0, 0, 0.4127)$ otherwise. The ratio of specific heat is $\gamma = 5/3$.

A big challenge for the computation is, negative pressure could appear if the PP limiter is not used since the internal energy is very small compared to the huge kinetic energy. The TVB limiter [9] is used before applying the PP limiter in each time stage to reduce the spurious oscillations where the density and pressure are far above zero, with the TVB constant $M = 10^5$. We compute the solution on the 320×160 grid, and show the density and pressure at $T = 5 \times 10^{-4}$ in Fig. 12. We can see good resolution in the picture comparable with the result in [48].

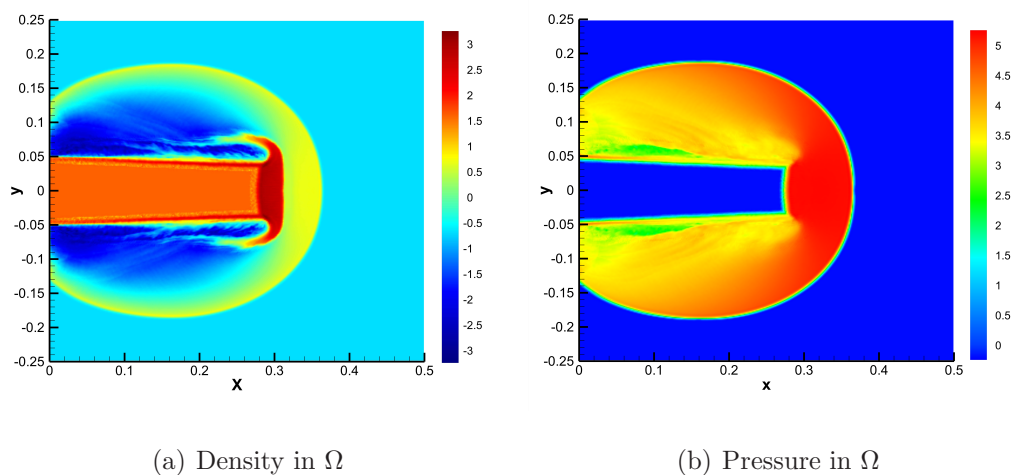


Figure 12: Results of Example 6.13 at $T = 5 \times 10^{-4}$ on the 320×160 grid.

7 Concluding remarks

In this paper, we have proposed a fourth order PP DG methods for scalar conservation laws and the compressible Euler equations of gas dynamics based on the SSP $S_2D_2O_4$ discretization. We have constructed a PP local LF type flux for the second temporal derivative terms, which satisfies the weak positivity property. No auxiliary variables are introduced other than the numerical solution, which saves computational costs. Besides, our algorithms are easy to be extended to higher-order accuracy. The main contribution of the paper is to prove rigorously that, under the suitable time-step conditions, the cell averages of the $S_2D_2O_4$ DG schemes at the next time step is positive, provided the specific variables of the solution are positive at the current time step. The PP limiter can then be used to enforce the positivity for the whole solution at the next time step. In the end, the fourth order accuracy and the PP property of the $S_2D_2O_4$ DG scheme are observed through extensive numerical experiments.

In our future work, we will consider to extend the algorithm to schemes with higher order accuracy. Also, it is important that we extend the algorithm to unstructured meshes.

References

- [1] R. Abedian and M. Dehghan, *The formulation of finite difference RBFWENO schemes for hyperbolic conservation laws: an alternative technique*, Adv. Appl. Math. Mech. 15 (2023) 1023-1055.
- [2] S. Busto, S. Chiocchetti, M. Dumbser, E. Gaburro and I. Peshkov, *High order ADER schemes for continuum mechanics*, Front. Phys. 8 (2020) 32.
- [3] Z. Chen, H. Huang and J. Yan, *Third order maximum-principle-satisfying direct discontinuous Galerkin methods for time dependent convection diffusion equations on unstructured triangular meshes*, J. Comput. Phys. 308 (2016) 198–217.

- [4] A.J. Christlieb, S. Gottlieb, Z. Grant and D.C. Seal, *Explicit strong stability preserving multistage two-derivative time-stepping schemes*, J. Sci. Comput. 68 (2016) 914-942.
- [5] B. Cockburn, S. Hou and C.-W. Shu, *The Runge-Kutta local projection discontinuous Galerkin finite element method for conservation laws IV: the multidimensional case*, Math. Comput. 54 (1990), 545-581.
- [6] B. Cockburn, S.-Y. Lin and C.-W. Shu, *TVB Runge-Kutta local projection discontinuous Galerkin finite element method for conservation laws III: one-dimensional systems*, J. Comput. Phys. 84 (1989) 90–113.
- [7] B. Cockburn and C.-W. Shu, *TVB Runge-Kutta local projection discontinuous Galerkin finite element method for conservation laws II: general framework*, Math. Comput. 52 (1989) 411–435.
- [8] B. Cockburn and C.-W. Shu, *The Runge-Kutta local projection-discontinuous-Galerkin finite element method for scalar conservation laws*, ESAIM: Math. Model. Numer. Anal. 25 (1991) 337–361.
- [9] B. Cockburn and C.-W. Shu, *The Runge-Kutta discontinuous Galerkin method for conservation laws V: multidimensional systems*, J. Comput. Phys. 141 (1998) 199–224.
- [10] J. Du and Y. Yang, *Maximum-principle-preserving third-order local discontinuous Galerkin method for convection-diffusion equations on overlapping meshes*, J. Comput. Phys. 377 (2019) 117-141.
- [11] M. Dumbser, C. Eaux and E.F. Toro, *Finite volume schemes of very high order of accuracy for stiff hyperbolic balance laws*, J. Comput. Phys. 227 (2008) 3971–4001.
- [12] M. Dumbser, F. Fambri, M. Tavelli, M. Badera and T. Weinzierl, *Efficient implementation of ADER discontinuous Galerkin schemes for a scalable hyperbolic PDE engine*, Axioms 7 (2018) 63.

- [13] M. Dumbser and M. Käser, *Arbitrary high order non-oscillatory finite volume schemes on unstructured meshes for linear hyperbolic systems*, J. Comput. Phys. 221 (2007) 693–723.
- [14] M. Dumbser and C.D. Munz, *Building blocks for arbitrary high order discontinuous Galerkin schemes*, J. Sci. Comput. 27 (2006) 215–230.
- [15] S. Gottlieb, D.I. Ketcheson and C.-W. Shu, *High order strong stability preserving time discretizations*, J. Sci. Comput. 38 (2009) 251–289.
- [16] S. Gottlieb, C.-W. Shu and E. Tadmor, *Strong stability-preserving high-order time discretization methods*, SIAM Rev. 43 (2001) 89–112.
- [17] W. Guo, J.-M. Qiu and J. Qiu, *A new Lax-Wendroff discontinuous Galerkin method with superconvergence*, J. Sci. Comput. 65 (2015) 299–326.
- [18] H. Hajduk, *Monolithic convex limiting in discontinuous Galerkin discretizations of hyperbolic conservation laws*, Computers & Mathematics with Applications 87 (2021) 120–138.
- [19] D. Kuzmin, *Monolithic convex limiting for continuous finite element discretizations of hyperbolic conservation laws*, Comput. Methods Appl. Mech. Engrg. 361 (2020) 112840.
- [20] A. Li, J. Li, J. Cheng, and C.-W. Shu, *High order compact hermite reconstructions and their application in the improved two-stage fourth order time-stepping framework for hyperbolic problems: two-dimensional case*, Commun.Comput. Phys. 36 (2024) 1-29.
- [21] C. Liang and Z. Xu, *Parametrized maximum principle preserving flux limiters for high order schemes solving multi-dimensional scalar hyperbolic conservation laws*, J. Sci. Comput. 58 (2014) 41–60.

- [22] D. Ling, J. Cheng and C.-W. Shu, *Conservative high order positivity-preserving discontinuous Galerkin methods for linear hyperbolic and radiative transfer equations*, J. Sci. Comput. 77 (2018) 1801–1831.
- [23] C. Liu, B. Riviere, J. Shen and X. Zhang, *A simple and efficient convex optimization based bound-preserving high order accurate limiter for Cahn–Hilliard–Navier–Stokes system*, SIAM J. Sci. Comput. 46 (2023) A1923-A1948.
- [24] S.A. Moe, A.R. James and D.C. Seal, *Positivity-preserving discontinuous Galerkin methods with Lax–Wendroff time discretizations*, J. Sci. Comput. 71 (2017) 44–70.
- [25] D. Pan, C. Zhong, C. Zhuo and S. Liu, *A two-stage fourth-order gas-kinetic scheme on unstructured hybrid mesh*, Comput. Phys. Commun. 235 (2019) 75-87.
- [26] L. Pan, K. Xu, Q. Li and J. Li, *An efficient and accurate two-stage fourth-order gas-kinetic scheme for the Euler and Navier–Stokes equations*, J. Comput. Phys. 326 (2016) 197–221.
- [27] T. Qin and C.-W. Shu, *Implicit positivity-preserving high-order discontinuous Galerkin methods for conservation laws*, SIAM J. Sci. Comput. 40 (2018) A81–A107.
- [28] J. Qiu, *A numerical comparison of the Lax-Wendroff discontinuous Galerkin method based on different numerical fluxes*, J. Sci. Comput. 30 (2007) 345–367.
- [29] J. Qiu, *Hermite WENO schemes with Lax-Wendroff type time discretizations for Hamilton-Jacobi equations*, J. Comput. Math. 25 (2007) 131–144.
- [30] J. Qiu, M. Dumbser and C.-W. Shu, *The discontinuous Galerkin method with Lax-Wendroff type time discretizations*, Comput. Methods Appl. Mech. Eng. 194 (2005) 4528–4543.
- [31] J. Qiu and C.-W. Shu, *Finite difference WENO schemes with Lax-Wendroff-type time discretizations*, SIAM J. Sci. Comput. 24 (2003) 2185–2198.

- [32] W.H. Reed and T.R. Hill, *Triangular mesh methods for the neutron transport equation*, Los Alamos Report LA-UR-73-479 (1973).
- [33] D.C. Seal, Y. Güçlü and A.J. Christlieb, *High-order multiderivative time integrators for hyperbolic conservation laws*, J. Sci. Comput. 60 (2014) 101–140.
- [34] L.I. Sedov, *Similarity and dimensional methods in mechanics*, Academic Press, New York, 1959.
- [35] C.-W. Shu, *TVB uniformly high-order schemes for conservation laws*, Math. Comput. 49 (1987) 105-121.
- [36] C.-W. Shu and S. Osher, *Efficient implementation of essentially non-oscillatory shock-capturing schemes*, J. Comput. Phys. 77 (1988) 439-471.
- [37] S. Srinivasan, J. Poggie and X. Zhang, *A positivity-preserving high order discontinuous Galerkin scheme for convection–diffusion equations*, J. Comput. Phys. 366 (2018) 120-143.
- [38] X. Tao, J.-M. Qiu and Z. Xu, *High order maximum-principle-preserving discontinuous Galerkin for convection-diffusion equations*, SIAM J. Sci. Comput. 37 (2015) A583-A608.
- [39] V.A. Titarev and E.F. Toro, *ADER: arbitrary high order Godunov approach*, J. Sci. Comput. 17 (2002) 609–618.
- [40] E.F. Toro, *Riemann solvers and numerical methods for fluid dynamics: a practical introduction*, Springer Science & Business Media 2013.
- [41] P.J. van der Houwen, *The development of Runge-Kutta methods for partial differential equations*, Applied Numerical Mathematics 20 (1996) 261-272.
- [42] J. J. W. van der Vegt, Y. Xia, and Y. Xu, *Positivity preserving limiters for time-implicit higher order accurate discontinuous Galerkin discretizations*, SIAM J. Sci. Comput. 41 (2019) A2037-A2063.

- [43] C. Wang, X. Zhang, C.-W. Shu and J. Ning, *Robust high order discontinuous Galerkin schemes for two-dimensional gaseous detonations*, J. Comput. Phys. 231 (2012) 653-665.
- [44] S. Wang and Z. Xu, *Total variation bounded flux limiters for high order finite difference schemes solving one-dimensional scalar conservation laws*, Math. Comput. 88 (2018) 691-716.
- [45] K. Wu and C.-W. Shu, *Geometric quasilinearization framework for analysis and design of bound-preserving schemes*, SIAM Rev. 65 (2023) 1031-1071.
- [46] T. Xiong, J.-M. Qiu and Z. Xu, *Parametrized positivity preserving flux limiters for the high order finite difference WENO scheme solving compressible Euler equations*, J. Sci. Comput. 67 (2016) 1066–1088.
- [47] Z. Xu, *Parametrized maximum principle preserving flux limiters for high order schemes solving hyperbolic conservation laws: one-dimensional scalar problem*, Math. Comput. 83 (2014) 2213-2238.
- [48] Z. Xu and C.-W. Shu, *Third order maximum-principle-satisfying and positivity-preserving Lax-Wendroff discontinuous Galerkin methods for hyperbolic conservation laws*, J. Comput. Phys. 470 (2022) 111591.
- [49] X. Zhang, *On positivity-preserving high order discontinuous Galerkin schemes for compressible Navier–Stokes equations*, J. Comput. Phys. 328 (2017) 301-343.
- [50] X. Zhang, Y. Liu and C.-W. Shu, *Maximum-principle-satisfying high order Finite volume weighted essentially nonoscillatory schemes for convection-diffusion equations*, SIAM J. Sci. Comput. 34 (2012) A627-A658.
- [51] X. Zhang and C.-W. Shu, *On positivity-preserving high order discontinuous Galerkin schemes for compressible Euler equations on rectangular meshes*, J. Comput. Phys. 229 (2010) 8918-8934.

- [52] X. Zhang and C.-W. Shu, *On maximum-principle-satisfying high order schemes for scalar conservation laws*, J. Comput. Phys. 229 (2010) 3091-3120.
- [53] Y. Zhang, X. Zhang and C.-W. Shu, *Maximum-principle-satisfying second order discontinuous Galerkin schemes for convection–diffusion equations on triangular meshes*, J. Comput. Phys. 234 (2013) 295-316.